

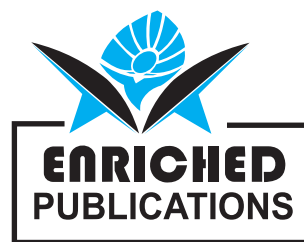
ISSN - 2683-3867

SERBIAN JOURNAL OF ELECTRICAL ENGINEERING

Volume No. - 21

Issue No. - 1

January - April 2024



ENRICHED PUBLICATIONS PVT. LTD

**JE-18, Gupta Colony, Khirki, Extn, Malviya
Nagar, New Delhi-110017**

PHONE : - + 91-8877340707

E-Mail : info@enrichedpublications.com

SERBIAN JOURNAL OF ELECTRICAL ENGINEERING

Aims & Scope

The Open Archives Initiative develops and promotes interoperability standards that aim to facilitate the efficient dissemination of content. The Open Archives Initiative has its roots in an effort to enhance access to e-print archives as a means of increasing the availability of scholarly communication. Continued support of this work remains a cornerstone of the Open Archives program. The fundamental technological framework and standards that are developing to support this work are, however, independent of the both the type of content offered and the economic mechanisms surrounding that content, and promise to have much broader relevance in opening up access to a range of digital materials. As a result, the Open Archives Initiative is currently an organization and an effort explicitly in transition, and is committed to exploring and enabling this new and broader range of applications. As we gain greater knowledge of the scope of applicability of the underlying technology and standards being developed, and begin to understand the structure and culture of the various adopter communities, we expect that we will have to make continued evolutionary changes to both the mission and organization of the Open Archives Initiative.

SERBIAN JOURNAL OF ELECTRICAL ENGINEERING

Managing Editor

Mr. Amit Prasad

Editor in chief:

Alenka Milovanović,

Faculty of Technical Sciences Čačak, University of Kragujevac, Serbia

alenka.milovanovic@ftn.kg.ac.rs

Editorial board

Gonzalo R. Arce,

University of Delaware, USA

Tadej Bajd,

Slovenian Academy of Sciences and
Arts, Slovenia

Hartmut Brauer,

Ilmenau University of Technology,
Germany

Ovidiu Florin Caltun,

Alexandru Ioan Cuza University of
Iasi, Romania

Yigang Cen,

Beijing Jiaotong University, China

SERBIAN JOURNAL OF ELECTRICAL ENGINEERING

(Volume No. - 21, Issue No. - 1, January - April 2024)

Contents

Sr. No.	Articles / Authors Name	Pg. No.
1	Low-Cost portable TRNG, Implementation and Evaluation - <i>Igor Fermevc1, Saša Adamović1</i>	1 - 8
2	Dynamic Modeling and Simulation of Power Transformer Maintenance Costs - <i>Olga Ristić1, Bratislav D. Iričanin2, Vladica Mijailović1</i>	9 - 22
3	Shielded Coupled Multilayered Microstrip Lines Analysis using HBEM - <i>Mirjana T. Perić1, Saša S. Ilić1, Slavoljub R. Aleksić1</i>	23 - 34
4	Analysis of the Impact of Network Architecture on Signal Quality in LTE Technology - <i>Ivana Stojanović1,2, Mladen Koprivica2, Nenad Stojanović3, Aleksandar Nešković2</i>	35 - 46
5	Modified Design of Microstrip Patch Antenna for UWB Applications - <i>Bashar Bahaa Qas Elias1, Haider Aljanabi2</i>	47 - 55

Low-Cost portable TRNG, Implementation and Evaluation

Igor Fermevc1, Saša Adamović1

ABSTRACT

This paper will show one of many possible hardware implementations of random sequence generators and give a short survey on existing work related to techniques used for producing true random bits. By using cheap electronic components found in every specialized store such as 8-bit RISC microcontroller, double analogue comparator chip and USB to RS232 interface integrated circuit, we were able to produce a low cost, highly portable device that outputs random sequences with excellent statistical characteristics and high entropy. The source of randomness is a mix of techniques such as electronic noise, phase noise and oscillator jitter. The device in question has a built-in debiasing algorithm similar to [1] and a security mechanism that protects the end user by constantly monitoring the quality of digitized noise signal. Finally, we will show the results of comparative analysis of data acquired from our device and „random.org“ online service.

Keywords: *Randomness, Electronic noise, Free running oscillator, Cryptography.*

1 About Randomness

Unpredictable and unrelated occurrences in nature or in a game of cards – randomness, chance or something else? Throughout the history, we have tried to explain, determine, predict or find a pattern in everything that surrounds us. Without going into religious or philosophical discussion on chance and randomness [2], we will stay in the field of mathematics and use Probability theory and Statistics to evaluate the level of randomness in data produced by random sequence generators. The assumption that only physical processes that occur in nature are totally unpredictable, unrelated or random, drives us to study and model the sources of randomness in such a way that they produce results which will be close to ones defined in [3]. By observing the wideband electronic noise signal, we can agree that its characteristics fulfill mathematically defined criteria for randomness, such as normal probability distribution of samples and uncorrelated sampled values. To prove this initial hypothesis in practice, we decided to produce a device that operates on these principals.

2 Previous Work

If we focus on possible types of randomness sources, as given in the survey on hardware random number generators [4] we can divide them in groups as shown in Fig. 1.

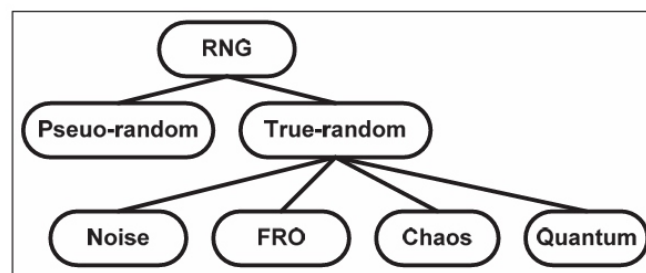


Fig. 1 – Types of randomness generators.

Although there is a large number of scientific papers and patents on the subject of hardware randomness generators, there is only a few practical implementations conforming to standards given by the NIST, BIS and other regulatory entities. State of the art generators known as quantum randomness generators are described in [5] and their price is in the range between one thousand and the tens of thousands USD which makes them inaccessible to most academic institutions. Next in line are generators working on principles described in [6] and we can summarize their block diagram of operation in a form shown in Fig. 2.



Fig. 2 – Block diagram of operation.

Our device follows the above block diagram and represents a mix of FRO and Noise based group of generators. Concerning its low price and characteristics it stands side by side to commercially available devices shown in Fig. 3. but as opposed to these there are no drawbacks to using unstable PN junction breakdown principle and no need to boost the voltage from USB power rail.

The comparative data for these devices are given in Table 1. As already stated, our device operates similar to a free running oscillator with variable pulse length and amplitude. These variations in signal are comparable to wideband white noise signal which gives us a good starting point for further processing.

One common feature with commercially available devices is USB interface which is accepted as a good idea because it allows the device to be portable and locally powered from the host computer. From the security and cryptographic perspective, the USB interface integrated circuit is the only part of the device that we must delegate the trust because we do not have the possibility to fully check all integrated components and features. One way to avoid this uncertainty is to implement USB stack and interface in microcontroller which would be a part of future work.

Table 1 TRNG characteristics.

Model	Speed [Kbs]	Randomness source	Power consumption [mW]	Price [USD]
Alea II	100	PN junction	250	150
TL200	2048	PN junction	100	200
True RNG2	350	PN junction	No data	50
One RNG	350	PN junction/RF noise	No data	50
Our device	72	FRO + El. noise	<100	20



Fig. 3 – Commercially available RNGs.

3 Implementation and Evaluation

3.1 Hardware Structure

The starting point for hardware development is the circuit diagram in Fig. 4. We have used the SMD electronic components with the intention of reducing the overall size of the device. The circuit is divided in segments that mimic the previously shown diagram. We start with a double analogue comparator LM393 which acts as noise source and digitizer. Microcontroller Atmel Attiny85 whose running code is written in AVR Assembler and processes the digitized signal, manages communication protocol and maintains the randomness pool. Final hardware segment is FTDI FT232RL integrated circuit used for interfacing the device through virtual serial port on host computer. We must point out that in order to evaluate certain security mechanism implemented in MCU running code all hardware safety measures have been avoided in the design. In order to use this device in real world applications, proper EMI shielding and additional power filtering circuits must be installed.

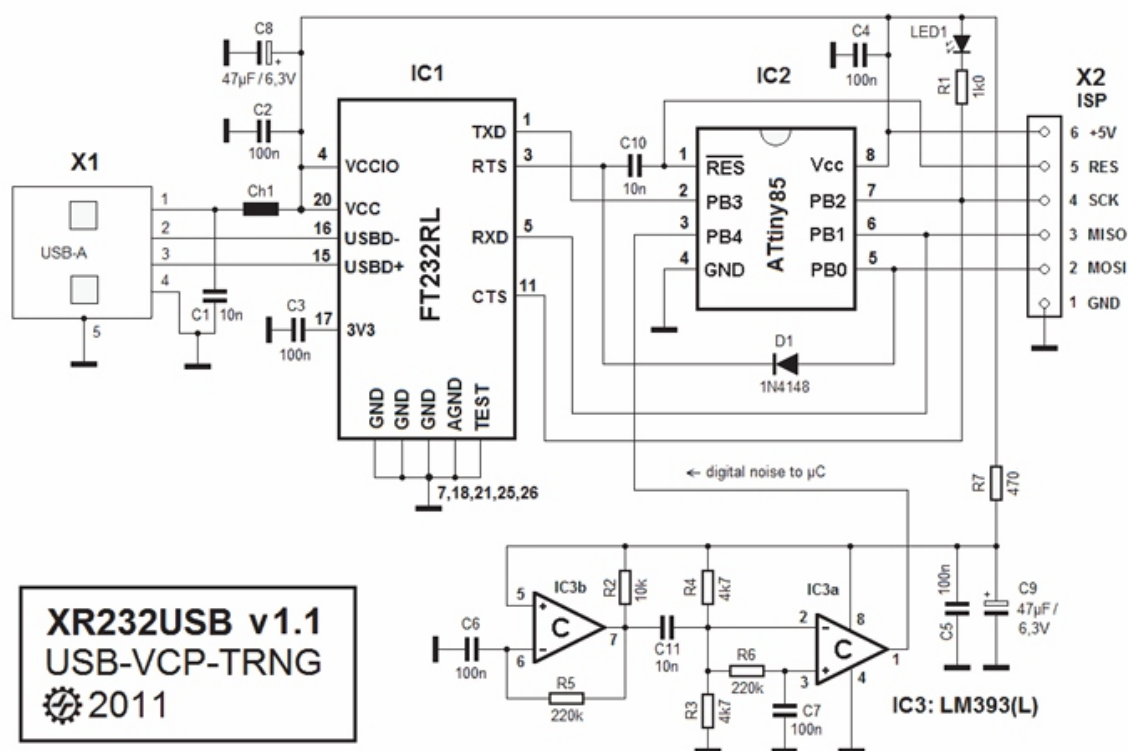


Fig. 4 – Circuit diagram [8].

3.2 Device Operation

Double analogue comparator LM393 serves two purposes. The first part of comparator is the source of nonlinearity. As stated in [7], in order to minimize multiple transitions in output when input signal is close to comparator threshold level, special attention must be paid while designing high speed comparator circuits. The right amount of hysteresis, feedback, good grounding, PCB layout, signal routing and decoupling are recommended techniques needed to avoid comparator output ringing. Opposite to best practices, lack of decoupling capacitors, possible stray capacitance and values of electronic components surrounding the first part of comparator chip resulted in, normally unwanted, erratic oscillations of output. Further examination of output signal demonstrated potentially good

random characteristics. The snapshot of noise signal acquired by DSO with its main characteristics is presented in Fig. 5. The second part of comparator works in standard mode. It compares the level of noise signal with reference voltage, amplifies the difference signal and converts it to a digital signal with variable period which is further routed to designated input of MCU. The simplified workflow diagram of MCU operation is shown in Fig.6.

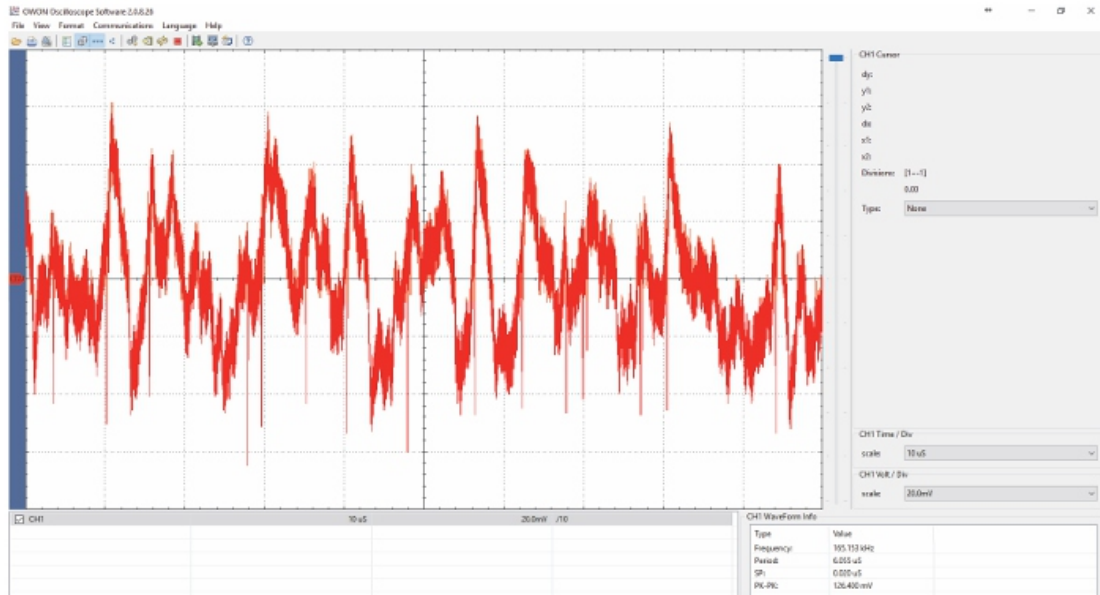


Fig. 5 – Wideband noise signal from the first part of comparator.

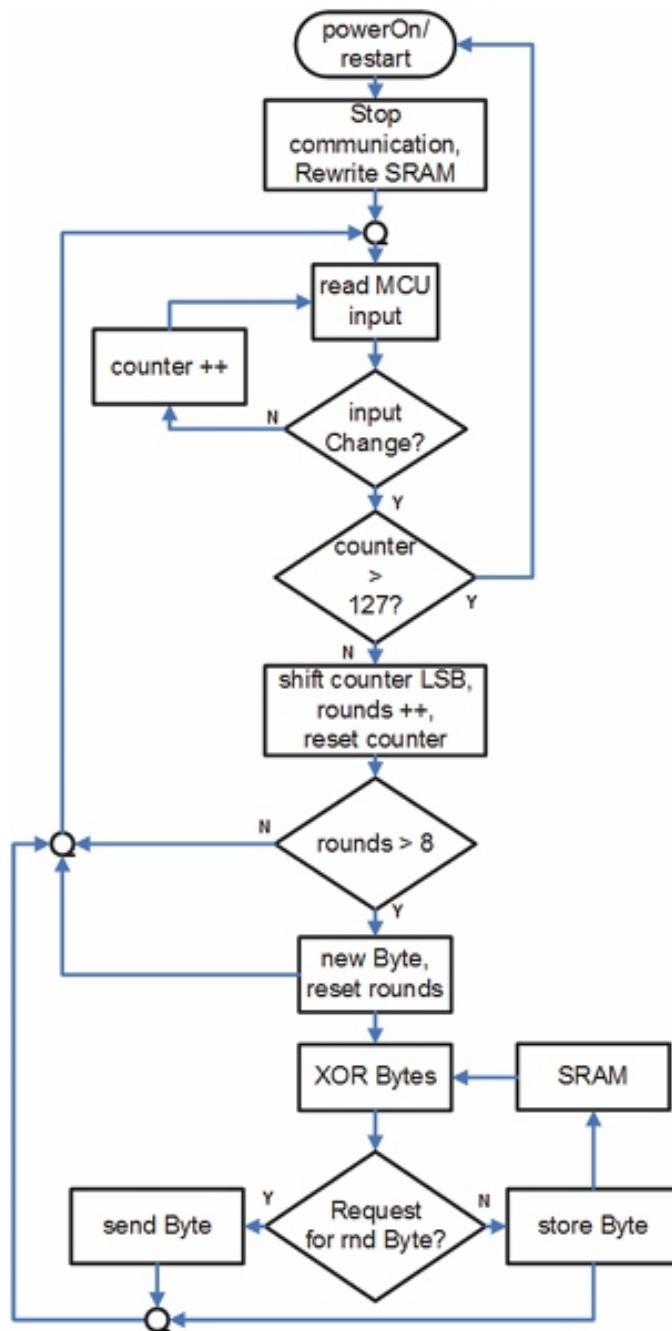


Fig. 6 – Simplified MCU workflow algorithm.

MCU running code is organized using macros. There is a separate macro for each state of RS232 handshake signals. Each macro executes the code for randomness pool maintenance incrementing the value of dedicated 8-bit register used as fast binary counter. By monitoring the digitized noise signal value on appropriate MCU input pin, counter is incremented until change in input signal is detected and the value of LSB in counter register is shifted into temporary register. We repeat this process until the whole byte is formed. The newly formed byte value along with previously stored byte is subjected to XOR operation. The resulting value is written into dedicated memory organized in a form of stack. The result of this operation is constantly refreshed pool of 500 random bytes. Because the value of binary counter is dependent on input signal period, if it exceeds certain value, we can assume that generated

bytes are not random and utilize this information to activate security macro which stops the serial communication and executes the MCU restart routine followed by emptying and refilling randomness pool. The time needed for MCU to distinguish random from nonrandom signal is not fixed and depends on many factors such as MCU clock speed, noise signal frequency and state of Rs232 signals.

3.3 Test Results

Evaluation of device operation is done using software application called XR232 [8] which implements the possibility to pull any number of random bytes from device and store them in a file. Collected data are then submitted to NIST statistical tests described in [9]. Apart from statistical test results, good properties of randomness can also be visualized as lack of pattern as shown in a Fig. 7.



Fig. 7 – Bitmap of random data sample.

We have also compared the statistical properties of the sequences produced by our generator and sample collected from “random.org” service, each consisting of 16 KB. The limitation in the amount of data is imposed by “random.org” service and the results are presented in Table 2.

Table 2. Comparative analysis of a couple of NIST test results ($P > 0.01$).

Test type		Our device	Random.org
Runs test (P)		0.439	0.0353
Serial test (P)	(P1)	0.390	0.087
	(P2)	0.858	0.665
Entropy test (bit)	Monobit	0.99999670	0.99997561
	Bigrams	0.99998785	0.99996795
	Trigrams	0.99998438	0.99996382
	Matrix 4x4	0.99997163	0.99995819

The results of statistical tests and comparative analysis proved our initial hypothesis that our device generates truly random bytes. To measure the speed of generation and delivery of the device we conducted an experiment a number of times in which we requested 1 MB of random data while

measuring the time.

Overall time was 114 seconds so we can conclude that device speed is 72 kbs. We have also simulated external interference by activating smart phone GSM or Wi-Fi transceiver near our device. If external disturbance is shorter than a couple of milliseconds, as measured with DSO and logic analyzer during the testing, data is delivered from randomness pool without interrupts in communication. Otherwise, the security routine is activated preventing delivery of no random, correlated data to user. Physical appearance of the device is shown in Fig. 8.

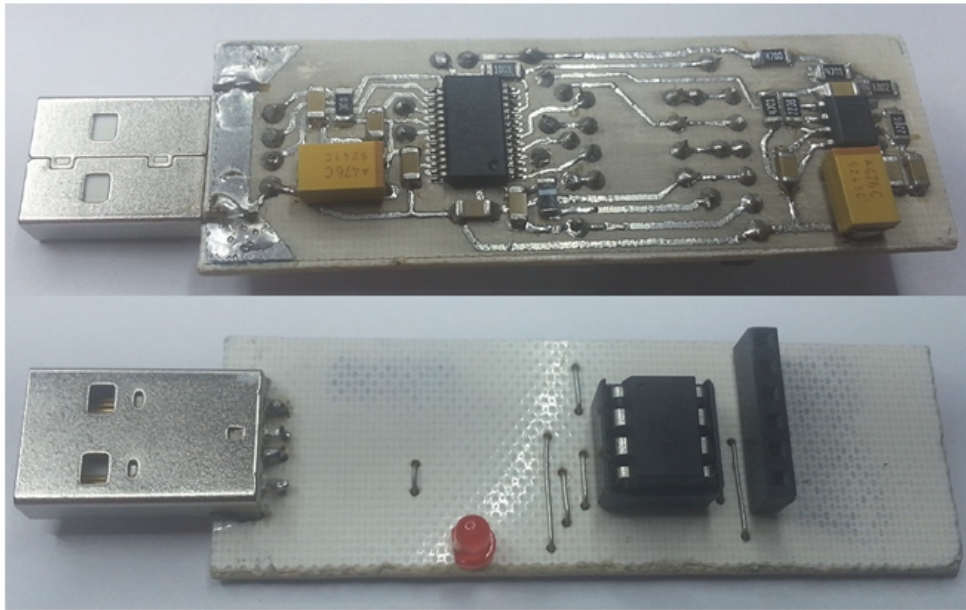


Fig. 8 – Physical appearance of our device.

4 Conclusion

We presented a theoretical concept of utilizing electronic noise as a source of randomness and constructed the hardware device to practically evaluate the properties of sequences it generates. We have also verified the quality of randomness source of our device by comparing its results to atmospheric noise based randomness generator. The results of statistical analysis confirmed extremely high level of entropy and unpredictability in produced sequences. We have also implemented and verified a real-time user protection security feature that enhances the trust in our device from cryptographic perspective. Compared to current state of the art quantum random generators the presented device is significantly slower but easy to produce, affordable and usable for various purposes, mainly as an educational tool. With minor modifications regarding EMI shielding and an increase in speed of delivery it can also be used in real life cryptography applications for generating sequences used as session keys for PGP, as strong passwords generator and many more.

5 References

- [1] J.V. Neumann: *Various Techniques used in Connection with Random Digits*, National Bureau of Standards Applied Mathematics Series 12, 1951, pp. 36–38.
- [2] A. Eagle: *Chance versus Randomness*, *The Stanford Encyclopedia of Philosophy*, 2016. Available at: <http://plato.stanford.edu/entries/chance-randomness/>.
- [3] W.B. Davenport Jr., W.L. Root: *An Introduction to the Theory of Random Signals and Noise*, John Wiley and Sons–IEEE Press, NY, USA, 1987.
- [4] M. Stipcevic, C.K. Koc: *True Random Number Generators*, C.K. Koc. (Ed.), *Open Problems in Mathematics and Computational Science*, Springer, 2014, pp 275–315.
- [5] J.F. Dynes, Z.L. Yuan, A.W. Sharpe, A.J. Shields: *A High Speed, Postprocessing Free, Quantum Random Number Generator*, *Applied Physics Letters*, Vol. 93, No. 3, July 2008, 031109.
- [6] W. Liao, M. Wan, K. Dai, X. Zou: *Scalable Truly Random Number Generator*, *World Congress on Engineering*, London, UK, 01-03 July 2015, Vol. 1.
- [7] R. Moghami: *Curing Comparator Instability with Hysteresis*, *Analogue Dialogue*, Vol. 34, No. 7, 2000, pp. 30–32.
- [8] J. Thomas: *XR232USB - True Random Numbers @ USB*. Available at: http://www.jtxp.org/tech/xr232usb_en.htm.
- [9] C. Kenny: *Random Number Generators: An Evaluation and Comparison of Random.org and Some Commonly used Generators*, *The Distributed Computing Group*, Trinity College Dublin, Ireland, April 2005.

Dynamic Modeling and Simulation of Power Transformer Maintenance Costs

Olga Ristić¹, Bratislav D. Iričanin², Vladica Mijailović¹

ABSTRACT

The paper presents the dynamic model of maintenance costs of the power transformer functional components. Reliability is modeled combining the exponential and Weibull's distribution. The simulation was performed with the aim of corrective maintenance and installation of the continuous monitoring system of the most critical components. Simulation Dynamic System (SDS) method and VENSIM PLE software was used to simulate the cost. In this way, significant savings in maintenance costs will be achieved with a small initial investment.

Keywords: *Modeling, Exponential and Weibull's distribution, Simulation, Power transformer, Maintenance.*

1 Introduction

Power transformers are one of the most important and critical components in the electric power distribution system. It is significant to determine the maintenance costs of power transformer and prevent the failure beforehand by applying preventive maintenance activities [1].

Dynamic modelling of power transformer maintenance activities based on different strategies of maintenance, determining the optimum moment of replacement elements, the spare parts purchases time, as well as minimizing the costs incurred in carrying out maintenance activities. Equipment behaviour is crucial for the implementation of preventive maintenance activities. In the dynamic modelling of power transformer reliability is necessary to establish a plan under which it shall be based on events and changes in the system, monitoring the state of certain elements, to determine the probability of component some failure generation.

For equipment that is being utilized for many years, modeling sets the minimum maintenance costs as well as interruptions in the supply of electrical energy (EE) to final consumers, according to [2, 3]. By analyzing the corrective maintenance strategies and continuous monitoring system instalation (CSMI) of critical elements in the example of a power transformer, it will be determined by combining the activities that aim to minimize costs and maximize power transformer availability [4].

In the recent years, for different types of calculation simulation that occur by numerical evaluation of model by the implementation of various software. The simulation can be used to predict system behaviour and optimization. In the paper will be apply the SDS method to simulate power transformer maintenance costs.

2 Model Development for Power Transformer Maintenance Activities

Failures that occur on the equipment in the most cases result deficits or interruptions in the delivery of EE to final consumers. The losses at the distribution company is proportional to the degree of equipment damage and to the cost of undelivered EE quantity. Consumer losses depending on the length and structure of the interruption of EE consumption. Failures that occur on power transformers cause the

most serious consequences because their removal takes time and costs. Therefore, right on their availability is an important technical and economic issue [5].

Failures can be repairable (avoidable) and unreparable (unavoidable). Elimination of power transformer avoidable failures takes a relatively short time and does not require spare parts. In order to remove unreparable failures spare parts ought to be used, so that the duration of failure elimination depends on their availability. Purchase of spare elements significantly influences the duration of the failure when it occurs, but this purchase requires substantial additional investments [6].

Power transformer has six functional components: windings and oil, core, bushings, tank, on-load tap-changer and other accessories. It can be in the operating or failure condition. Failure condition of power transformer conversion can be divided into minor failures and major failures, which occur due to the loss of one or more of transformer functionality. Failures which can be removed for a period shorter than one day belong to minor failures. Probability that component "k" of power transformer is in operating state is presented through the combination of exponential and Weibull distribution [7]:

$$R_k(t) = \exp(-(\lambda_{k,mf} + \lambda_{k,MF})t) \exp\left(-\left(\frac{t}{\alpha_k}\right)^{\beta_k}\right), \quad (1)$$

where:

t - time,

, k k

- Weibull scale and shape parameter for component " " k , respectively,

, kMF

and , kmf

are major and minor failure rate of component " " k , respectively.

According to the expected duration of failure renewal time, there are three categories of failures [8]:

failures which can be repaired for 1 t day,

failures which can be repaired for 1 30 t days,

failures that can be repaired for 30 t days.

The maintaining activities of power transformer may be considered depending on the implemented measures [7, 8] and can be carried out through:

1) corrective maintenance,

2) one-day maintenance,

3) oil regeneration,

4) insulation system regeneration,

5) power transformer refurbishment,

6) CMSI,

7) spare equipment optimization.

At this point, we shall consider only the case of extreme values of costs. More specifically, these are the costs of corrective maintenance and installation of continuous monitoring system (CMS) on power transformer elements.

2.1 Cost estimation model for corrective maintenance

The corrective maintenance is carried out in the case of operation without spare equipment or

maintenance. In the planning period of exploitation costs, only the renewal costs will be included. During the period $[t, t+1]$ estimated annual value of these costs per transformer, can be calculate from the expression [7]:

$$C_{PT,b}(t, t+1) = \frac{[R_{tot}(t) - R_{tot}(t+1)] \sum_{k=1}^b p_k \left(\sum_{i=1}^{f_k} p_{k,i} C'_{k,i} \right)}{\int_t^{t+1} R_{tot}(t) dt + [R_{tot}(t) - R_{tot}(t+1)] \sum_{k=1}^b p_k \sum_{i=1}^{f_k} p_{k,i} r'_{k,i}},$$

$$R_{tot}(t) = \prod_{k=1}^b R_k(t), \quad (2)$$

where:

$p_{k,i}$

C - renewal cost of class i failure on component k if spare component k is not available,
 R_{tot} - reliability function of power transformer,

R_k - reliability function of power transformer component,

p_k - probability that the failures occurs on power transformer component k ,

f_k - number of failure classes of power transformer component k , regard to the failure repair time,

$p_{k,i}$ - probability that the failure of category i show in component k ,

$r_{k,i}$ - renewal time of category i occurs of component k if spare component k is not available,

$r'_{k,i}$ - renewal time of category i occurs of component k if spare component k is available,

b - number of functional components of power transformer.

2.2 CMSI cost model

The expected service life of the commercially available CMS is 10 years, and the purchase price is about 10% of the corresponding components purchase price. In the literature, the price and duration of detected faults mostly are ignored, because it is minimal or zero. For safety reasons, it is assumed that the detected defects in the windings and core eliminated in 5 days at a price of 5000 EUR, while on the other components will be eliminated only minor failures. By CMSI of power transformer components enables detection of failures at the earliest stage of development. This increases the intensity of minor and reduces the intensity of major component failures. Reducing the intensity of major failures has resulted in an increase in scale parameter of Weibull's distribution.

If we denote with $\alpha'_k, k=1,2$, scale parameter of winding and core after CMSI, CMS will be installing after T_S year of exploitation without failure. If transformer will not fail for next 10 years of exploitation reliability will be change according to expression

$$R'_{tot}(t) \approx R_1(T_S) R_2(T_S) R'_1(t - T_S) R'_2(t - T_S) \prod_{k=3}^b R_k(t), \quad (3)$$

$$R'_k(t - T_s) = \exp\left[-(\lambda'_{k,MF} + \lambda'_{k,mf})(t - T_s)\right] \exp\left[-\left(\frac{t - T_s}{\alpha'_k}\right)^{\beta_k}\right], \quad k = \overline{1,2}.$$

Expected costs in the first year after first CMSI are calculated as:

$$C_{PT,CMS}(T_s, T_s + 1) = \frac{X \left(\sum_{j=1}^2 P_j \sum_{i=1}^{f_j} P_{j,i}^{CMS} C_{j,i}^{CMS-b} + \sum_{k=3}^b P_k \sum_{i=1}^{f_k} P_{k,i} C'_{k,i} \right)}{\text{Im}_{CMS}(T_s, T_s + 1)} +$$

$$+ \frac{R_{tot}(T_s) C_{s,1-2}}{Y \left(\sum_{j=1}^2 P_j \sum_{i=1}^{f_j} P_{j,i}^{CMS} r_{j,i}^{CMS-b} + \sum_{k=3}^b P_k \sum_{i=1}^{f_k} P_{k,i} r'_{k,i} \right)} + C_{m-CMS}, \quad (4)$$

$$X = (R'_{tot}(T_s) - R'_{tot}(T_s + 1)), Y = \int_{T_s}^{T_s+10} R'_{tot}(t) dt + (R'_{tot}(T_s) - R'_{tot}(T_s + 10)),$$

$$\text{Im}_{CMS}(T_s, T_s + 1) = \int_{T_s}^{T_s+1} R'_{tot}(t) dt + (R'_{tot}(T_s) - R'_{tot}(T_s + 1)) \cdot$$

$$\cdot \left(\sum_{j=1}^2 P_j \sum_{i=1}^{f_j} P_{j,i}^{CMS} r_{j,i}^{CMS-b} + \sum_{k=3}^b P_k \sum_{i=1}^{f_k} P_{k,i} r'_{k,i} \right),$$

where:

, CMS b k i C - renewal cost of category “i” on component “k” of power transformer if CMS is installed and component “k” is not available,

, CMS b k I r

- renewal time of category “i” on component “k” of power transformer if CMS is installed and component “k” is not available,

, k i CMS p - probability that the failure of class “i” occurs on power transformer component “k” after installing CMS,

mCMS C

- annual maintenance cost of CMS.

3 Power Transformer Cost and Failure Data Analysis

The CMSI will certainly decrease maintenance costs. In recent years, with the development of different types of sensors and information technology, it is possible to reduce preventive maintenance activities. If any changes in the equipment occurrence, it will provide data that indicate the need for preventive interventions. Therefore, it is considered to be the optimal time for installing CMS at every critical element of the power transformer, and then the costs would be minimal [9, 10].

In Table 1 the data of component contribution in total number of failures of power transformers are given, as well as the duration of certain failures categories elimination. The values of the degree of detected faults are listed in Table 2. In the same table is the purchase price of components and power transformer 110kV, 110/x kV/kV, 31,5MVA.

Table 1 Power transformer component reliability data and removal duration of certain categories failures [7].

Component	$p_k, \%$	Failure "category" by duration	$p_{k,i}, \%$	$r'_{k,i}$	$r''_{k,i}$
1) Windings + oil	26,4	≤ 30 days	14,54	30	15
		> 30 days	85,46	250	15
2) Core	2,4	1÷30 days	50,00	30	15
		> 30 days	50,00	180	15
3) Bushing	12,0	≤ 1 day	14,82	1	1
		1÷30 days	51,85	40	3
		> 30 days	33,33	40	15
4) Tank	7,9	≤ 1 day	58,82	1	1
		1÷30 days	23,53	3	3
		> 30 days	17,65	90	15
5) On-load tap-changer	40,7	≤ 1 day	25,61	1	1
		1÷30 days	52,44	3	3
		> 30 days	21,95	40	3
6) Other accessories	10,6	≤ 1 day	65,22	1	1
		1÷30 days	17,39	15	15
		> 30 days	17,39	40	15

It is adopted that the price of undelivered EE $C_{PT} = 0,10$ EUR/kWh, time of refurbishment $t_{ref} = 28$ days, price of filtration and drying oil $C_{oil-fd} = 0,2C_{new,oil}$, price of one-day maintenance $C_{one-day} = 100$ EUR, cost of oil regeneration $C_{reg.-oil} = 8000$ EUR, price of insulation regeneration $C_{reg.-ins} = 100000$ EUR, probability of reduction "technical age" of paper isolation $x = 0,3$.

Purchasing cost of CMS is 10% of component price on which CMS will be installing: $C_{s,k} = 0,1C_{new,k}$. Annual maintenance cost of CMS is 1% of

purchasing price. In Table 3 are presented the prices of failure renewal cost on power transformer components.

Table 2. Values for detection rate and price of new elements of power transformer 110/x kV/kV.

Component	The level of detection d_k [%]	Cost of purchase new component $C_{new,k}$ [EUR]
Windings + oil	70	250 000+ 40 000
Core	70	80 000
Bushing	80	800
Tank	-	28 000
On-load tap-changer	75	42 000
Other accessories	100	22 000

Table 3. Failures renewal costs for power transformer components

Component	p_k , %	Failure "category" by duration	Failure renewal cost without spares $C_{k,i}$	Failure renewal cost with available spares $C_{k,i}^*$
1) Windings + oil	26,4	≤ 30 days	$0,2C_{new,1} + C_{ii}$	C_{ii}
		> 30 days	$0,5C_{new,1} + C_{ii}$	C_{ii}
2) Core	2,4	$1 \div 30$ days	$0,2C_{new,2} + C_{ii}$	C_{ii}
		> 30 days	$0,5C_{new,2} + C_{ii}$	C_{ii}
3) Bushing	12,0	≤ 1 day	$0,4C_{new,3}$	$0,4C_{new,3}$
		$1 \div 30$ days	$C_{new,3}$	-
		> 30 days	$C_{new,3} + C_{ii}$	C_{ii}
4) Tank	7,9	≤ 1 day	$0,1C_{new,4}$	$0,1C_{new,4}$
		$1 \div 30$ days	$0,2C_{new,4}$	$0,2C_{new,4}$
		> 30 days	$C_{new,4} + C_{ii}$	C_{ii}
5) On-load tap-changer	40,7	≤ 1 day	$0,1C_{new,5}$	$0,1C_{new,5}$
		$1 \div 30$ days	$0,2C_{new,5}$	$0,2C_{new,5}$
		> 30 days	$0,4C_{new,5}$	-
6) Other accessories	10,6	≤ 1 day	$0,1C_{new,6}$	$0,1C_{new,6}$
		$1 \div 30$ days	$0,5C_{new,6}$	$0,5C_{new,6}$
		> 30 days	$C_{new,6}$	-

The application of the proposed model is illustrated in the case of a power transformer' station (TS) 110/x kV/kV, where two 31,5MVA power transformers are installed. Linearized diagram of annual duration of the load for the analyzed TS is shown in Fig. 1 [8]. Maximum load is 80% and minimum 40% of installed capacity, where instal $P_{instal} = 231,5$ 63MVA.

The parameters of distributions were determined based on the data exploitation of the annual intensity of

power transformers major failures in the United States (Fig. 1). For adopted mean failure intensity $\lambda_{av} = 0.015$ year of the power transformer for the first 30 years of exploitation, based on the curve of Fig. 1 and the data given in Table 1, using the least-squares method is obtained parameters of the Weibull distribution for individual components (Table 4). In the same table is presented lists of the parameters values in case if at each component individually installed CMS, based on data from Table 1 and Table 2 [7, 11].

4 Modelling the Structure of the System Using SDS Method

SDS is used for modelling and simulation of complex dynamic systems with different computer programs [12]. There is a significant application in the analysis of complex dynamic systems, where it is possible to determine what the effects obtained on the system when making certain decisions. By creating SDS model, it is important to understand the causes and consequences of the problem which will be modelling. After the behavior of the system has been examined, dependences between the components in the system will be determined. This method was applied to different kinds of systems: social, environmental, manufacturing, service, biological, agricultural, health, etc. SDS model should have the following characteristics [13]:

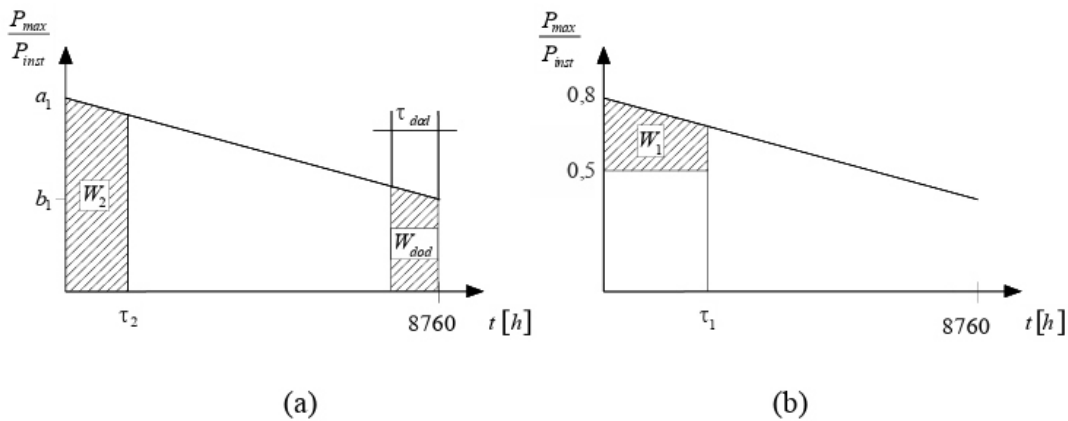


Fig. 1 – Annual linearized load-duration diagram ($a_1 = 0,8; b_1 = 0,4$).

describe any problem with the cause - consequence relations, the application of mathematical formulas in the simulation system,

the possibility of applying a large number of variables,

the analysis of data obtained by simulating a change in the decision.

Each model represents a simplification of the system. To be useful, it does not reflect the system in detail and will depend on the application of the model to solve a problem. The model needs to determine the most important elements of the system. This means simplifying the model, which will not be too complex for the purpose of practical analysis. These models have certain limitations with respect to inaccuracy and errors that can occur due to incorrectly create model.

Table 4 Weibull distribution parameters for components

k	Component	β_k	Without CMS α_k	CMS is available α'_k
1	Windings + oil	3,58	57,013	79,805
2	Core	3,58	111,395	155,927
3	Bushing	3,58	74,316	116,500
4	Tank	3,58	102,321	102,321
5	On-load tap-changer	3,58	54,872	80,213
6	Other accessories	3,58	98,808	∞

When applying SDS method for the complex systems behavior analysis, there is commonly used modeling software such as: ARENA, OPEN MODELICA, DYNAMO, DYSMAP, ITHINK/STELLA, POWERSIM, VENSIM, etc.

4.1 VENSIM PLE software for system dynamic modeling

VENSIM PLE software is used for visual modeling that allows creating the models, documentation, system analysis, simulation and optimization of created dynamic systems models. This software tool developed by “Ventana Systems” in 1985 for solving management problems by using simulation [14]. On Fig. 2 provides an overview of the software-working environment. The advantage of this software is that it allows calling external function (programmed in any programming language) that will be used for simulation model. It is possible to import models that were created in other software (such as MATLAB) used for modeling and simulation and adapt for their own needs. In the models are created different dependencies between variables. Based on defined models it can be made simulations of various events. The model in this software can create as Stock and Flow Diagram (SFD). SFD is used for displaying the system behavior and the relationship between the variables in the system. Based on these diagrams, the state of the system is determined, as well as the received information on which decisions are being made.

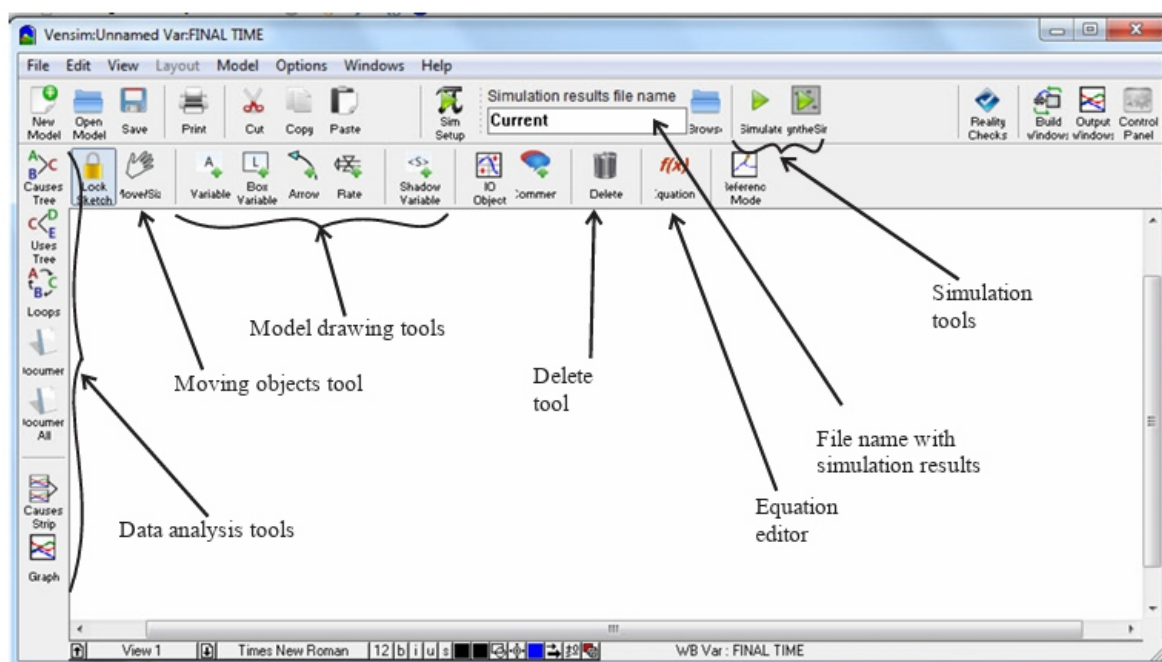


Fig. 2 – VENSIM PLE working environment.

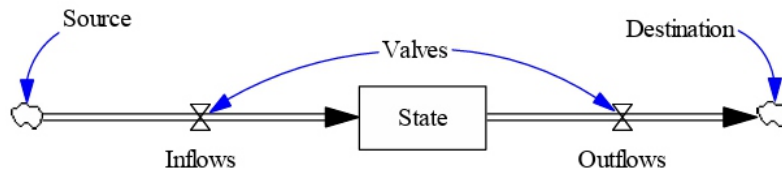


Fig. 3 – The SFD elements.

The first step of the simulation model is creating this diagram. A certain value has to be assigned to every variable, and formulas important for describing the system behavior should be defined. In the SFD, a dynamic model of the system is represented by the elements shown in Fig. 3. The basic elements of SFD are as follows [15]:

Rectangle – shows different states in time t .

Inflows - thicker arrows that enter into rectangle (increases parameters of defined state).

Outflows - coming out of rectangle and represent changes in the state for a time interval $(t, t + dt)$ (reduced values of the state parameters).

Valves - designation that controls input and output variables.

Clouds - represent sources and destinations of information flows.

Source represents the state from which the model appears, and destinations represent a state of in which information is collected.

4.2 SFD of power transformers maintenance costs

When SFD model has been created at the beginning, it must define the initial model parameters.

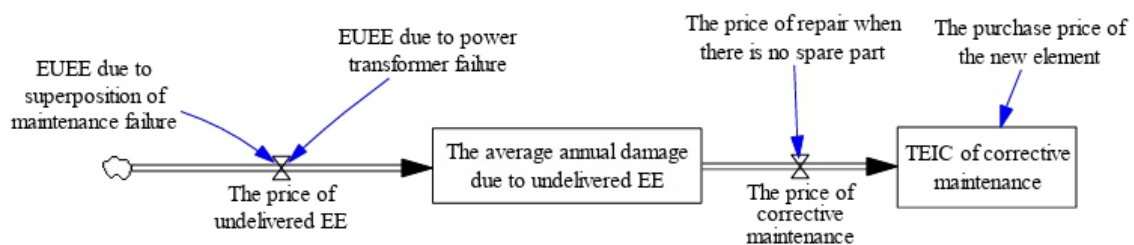


Fig. 4 – SFD of power transformer corrective maintenance costs.

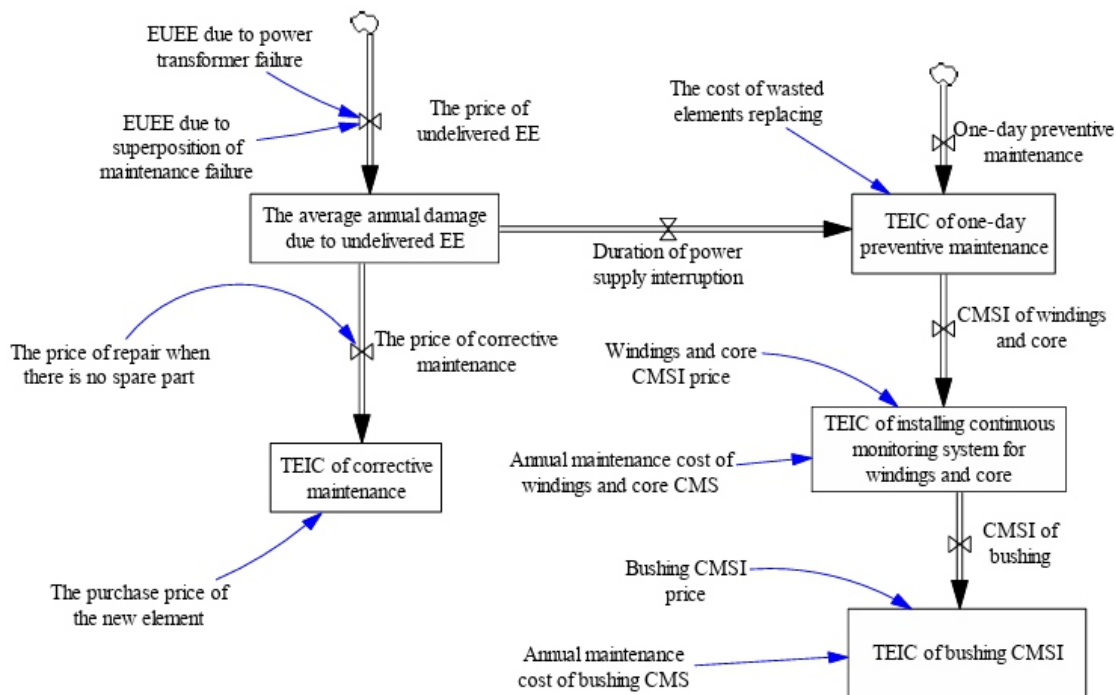


Fig. 5 –SFD of power transformer maintenance costs in case of CMSI.

For power transformer cost model, the time is displayed in the years and exploitation-planning period of 40 years has been adopted. Based on the proposed model, diagrams of power transformer maintenance costs are designed depending on the type of maintenance that is carried out [16]. SFD of power transformer maintenance costs are showing in Fig. 4 in case of corrective maintenance, and Fig. 5 for the case of installing the CMS.

Abbreviations used in the following figures are:

TEIC – Total Expected Interruption Costs,

EUEE – Expected Undelivered Electrical Energy.

4.3 Simulation of power transformer total expected exploitation costs using Vensim software

To perform a simulation of created model that is represented by the SFD, it is essential to enter correct formula for each using Equations icon. The editor is obtained by clicking on any variable as shown in Fig. 6. In the editor section Variable Information is enter basic information such as Name, Type, Units, etc. Equations could be entered into the middle part of editor, labeled as Equations where it is possible to use the system defined function given in section Functions.

If the user enters the wrong name of variable or formula in section Errors it will be reported errors review. Sections Check Syntax and Check Model test the syntax of the given equations and models and perform simulation. If there is any error, the simulation will not start until the error is corrected.

The values that are obtained by simulating the costs could be presented with tools which are found on the right side of the working environment. Fig. 7 shows the graph which simulates the expected total costs of corrective maintenance for planned exploitation period of 40 years. The implementation of this strategy of maintaining obtains the maximum maintenance costs.

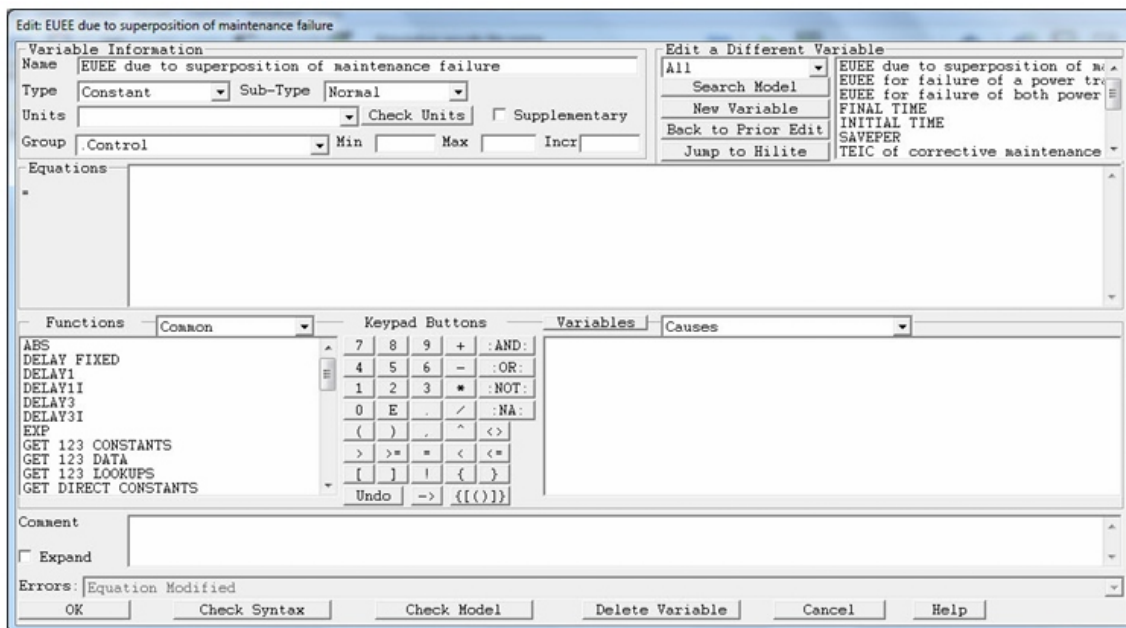


Fig. 6 – Equation editor for entering formulas and variables.

Installation CMS of windings and core is justified from the first year of power transformer exploitation. They will be installed at every ten years, as follows: at the beginning of 11th, 21st and 31st exploitation year. Installation CMS of bushings shall be from first exploitation year. It is important to point out that after the implementation of these activities during the planning period of 40 years, it is not justified to implement a one-day maintenance, nor oil regeneration, nor insulation system regeneration. It remains to analyze the justification of spare parts purchase and implementation of power transformer revitalization.

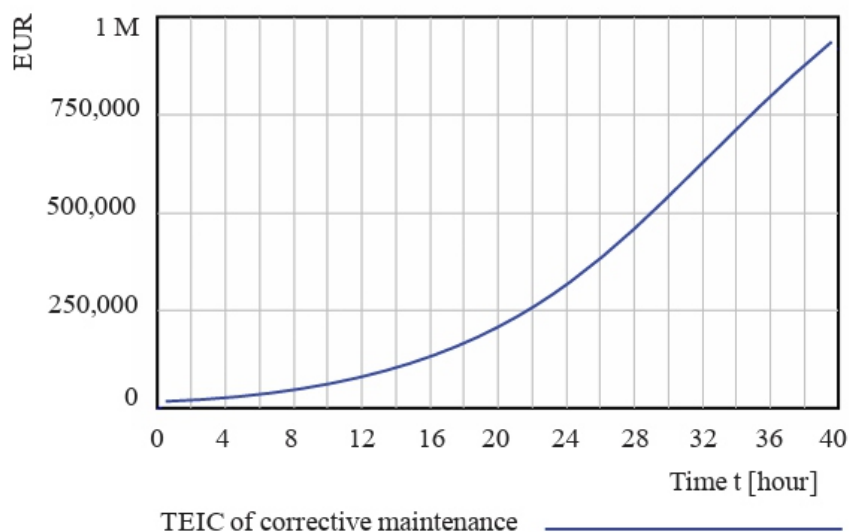


Fig. 7 – Simulation graph of power transformer total expected maintenance costs in a case of corrective maintenance.

Gradual analysis has simply calculated that it is justified to obtain spare part of:

tap charger from the beginning of the 9th year,

windings since the beginning of the 10th year,

tank from the beginning of 14th years,

other equipment from the beginning of 15th years and implement the revitalization of the transformer at the beginning of 25th year [7].

In this way, there is no need for the acquisition of the spare core. Simulation of power transformer minimum total expected maintenance costs are obtained in the case of implementing series of activities that are shown in Fig. 7. Here are used VENSIM PLE software tools for drawing these diagrams. On Fig. 8 is presented simulation of costs by installing a system for continuous monitoring of windings, core, bushings and revitalization of power transformer at the beginning of 25 years of exploitation.

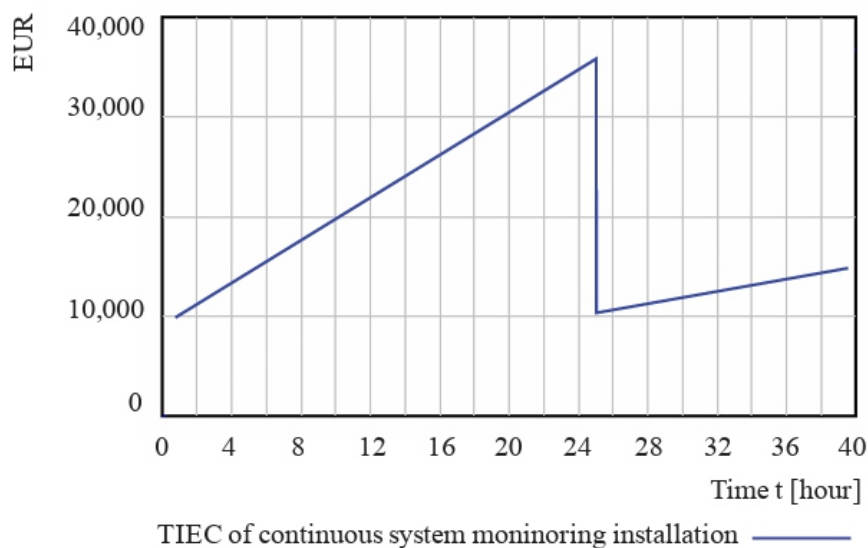


Fig. 8 – Simulation graph of power transformer minimal total expected maintenance costs.

5 Conclusion

The importance of the defined dynamic model is to determine the costs that are incurred upon the supplier of EE and consumers due to the failures occurrence. The implementation of preventive activities such as installing CMS on the transformer components is intended to carry out minimization of costs and increase equipment availability. In addition to these preventive activities can be carried out number of other activities such as spare parts purchasing, the revitalization of transformers, oil changes, etc. All these activities are aimed at reducing costs due to unavailability and increase power transformer exploitation life [17].

Application of the SDS method at cost simulation aims to identify extreme minimum and maximum maintenance costs without the use of a reserve power transformer.

6 Acknowledgement

The second author is partially supported by the by the Serbian Ministry of Science, projects III 41025 and OI 171007.

7 References

- [1] J. Nahman, V. Mijailović: *Selected Chapters from the High-Voltage Switchgears*, Akademska misao, Belgrade, Serbia, 2002. (In Serbian).
- [2] J. Nahman, V. Mijailović: *Reliability of Electrical Distribution System*, Akademska misao, Belgrade, Serbia, 2009. (In Serbian).
- [3] A. van Schijndel: *Power Transformer Reliability Modelling*. PhD Thesis, University of Technology, Eindhoven, The Netherlands, 2010.
- [4] H. Ge: *Maintenance Optimization for Substations with Aging Equipment*, PhD Thesis, University of Nebraska–Lincoln, Lincoln, NE, USA, 2010.
- [5] G. Nourbakhsh: *Reliability Analysis and Economic Equipment Replacement Appraisal for Substation and Sub-Transmission Systems with Explicit Inclusion of Non-Repairable Failures*, PhD thesis, Queensland University of Technology, Queensland, Australia, 2011.
- [6] A. van Schijndel, P.A.A.F. Wouters, E.F. Steennis, J.M. Wetzer: *Approach for an Integral Power Transformer Reliability Model*, *European Transactions On Electrical Power*, Vol. 22, No. 4, May 2012, pp. 491 – 503.
- [7] O. Ristic, V. Mijailovic: *Method for Determining Optimal Power Transformers Exploitation Strategy*, *Electric Power Systems Research*, Vol. 83, No. 1, Feb. 2012, pp. 255 – 261.
- [8] V. Mijailovic: *Method for Effects Evaluation of Some Forms of Power Transformers Preventive Maintenance*, *Electric Power Systems Research*, Vol. 78, No. 5, May 2008, pp. 765 – 776.
- [9] V. Mijailovic: *Optimal Spares Availability Strategy for Power Transformer Components*, *Electric Power Systems Research*, Vol. 80, No. 8, Aug. 2010, pp. 987 – 992.
- [10] R.A. Jongen, E. Gulski, P.H.F. Morshuis, J.J. Smit, A.L.J. Janssen: *Statistical Analysis of Power Transformer Component Life Time Data*, *8th International Power Engineering Conference*, Singapore, 03-06 Dec. 2007, pp. 1273 – 1277.
- [11] A. van Schijndel, J.M. Wetzer, P.A.A.F. Wouters: *Remaining Lifetime Modelling for Replacement of Power Transformer Populations*, *International Conference on Condition Monitoring and Diagnosis*, Beijing, China, 21-24 April 2008, pp. 597 – 600.
- [12] J. Sterman: *Business Dynamics Systems Thinking and Modeling for a Complex World*, Irvin - McGraw Hill Higher Education, ISBN 0 - 07 - 231135 - 5, 2000, 982 p.
- [13] E. Kremers: *Modelling and Simulation of Electrical Energy Systems through a Complex Systems Approach using Agent-Based Models*, PhD Thesis, KIT Scientific Publishing, Karlsruhe, Germany, 2013.
- [14] <http://vensim.com/>
- [15] P. Basirat, H. Fazlollahtabar, I. Mahdavi: *System Dynamics Meta-Modelling for Reliability Considerations in Maintenance*, *International Journal of Process Management and Benchmarking*, Vol. 3, No. 2, 2013, pp.136 – 153.
- [16] R. Chumai: *System Dynamic Modeling of Plant Maintenance Strategy in Thailand*, *27th International Conference of the System Dynamics Society*, Albuquerque, NM, USA, 26-30 July 2009.
- [17] O. Ristić: *Dynamic Modeling and Simulation of Preventive Exploitation Activities in Electric Equipment Reliability Analysis*, PhD Thesis, University of Kragujevac, Serbia, June 2016. (In Serbian).

Shielded Coupled Multilayered Microstrip Lines Analysis using HBEM

Mirjana T. Perić¹, Saša S. Ilić¹, Slavoljub R. Aleksić¹

ABSTRACT

Shielded symmetrical coupled multilayered microstrip lines analysis have been done using the hybrid boundary element method (HBEM), which is developed a few years ago at the Faculty of Electronic Engineering in Niš. The quasi-TEM approximation is applied. Influences of different parameters as well as dimensions of such microstrip lines on characteristic parameters distribution are investigated. The results are presented in graphs and tables. In order to verify the obtained results, some comparative results are shown. The authors found them to be in very good agreement with the HBEM results.

Keywords: *Characteristic parameters, Finite element method, Hybrid boundary element method, Multilayered structures, Shielded coupled microstrip lines.*

1 Introduction

Scientists and researchers in the world, during the past six decades, try to develop methods that produce enough accurate and precise results for microstrip lines characteristic parameters. Different configurations are subject of many papers. Also, different methods have been developed and applied. List of commonly used methods for microstrip lines analysis is very wide, but here it can be mention some of them such as the variational method [1], the boundary element method (BEM) [2, 3], the finite element method (FEM) [4, 5], the finite difference method (FDM) [6], the equivalent electrodes method (EEM) [7], etc. Most of those methods, in different manners, calculate the capacitance per unit length of the analysed microstrip line. After that, it is possible to obtain the effective permittivity, ϵ_r^{eff} , and characteristic impedance, Z_c expressions, given in (1) and (2), respectively:

$$\epsilon_r^{\text{eff}} = \frac{C'}{C_0}, \quad (1)$$

$$Z_c = \frac{1}{c\sqrt{C'C_0}} = \frac{Z_{c0}}{\sqrt{\epsilon_r^{\text{eff}}}}, \quad (2)$$

where $C = 3 \cdot 10^8$ m/s c is the speed of light and C' is the capacitance per unit length of the microstrip line. C_0 and Z_{c0} are the capacitance per unit length and characteristic impedance of the same microstrip line when the microstrip is airfilled (the dielectric layers are replaced by air), respectively. The hybrid boundary element method (HBEM), described in detail in [8] and [9], is suitable and effective as other numerical methods for microwave transmission lines analysis.

The HBEM is based on the BEM, on the EEM, on the point-matching method (PMM) for the potential of the perfect electric conductor (PEC) electrodes and for the normal component of the electric field at the boundary surface between any two dielectric layers. Open structures, covered and coupled microstrip lines were until now researched using the HBEM, [8 – 14]. In this paper, the method is applied for characteristic parameters determination of shielded coupled multilayered microstrip lines. The calculation is based on a quasi-static TEM approach. This approach involves an evaluation of microstrip

lines as transmission lines of parallel plates, which support a quasi TEM mode of propagation. As basic components for directional couplers design, band-pass filters, delay lines, semiconductor devices, etc. are used coupled microstrip lines. The conductor metallization thickness has an influence on the microstrip lines characteristic parameters. It should be mention that this effect is more noticeable for the coupled microstrip lines then for the single. The PMM, used in [15], analyses the shielded microstrip lines with the finite metallization thickness. In [16] the authors state that the PMM gives acceptable results only if parameter t/w is smaller than 0.01. An extended point-matching method is developed in [16] to analyse microstrip lines with thick electrodes. The HBEM results obtained for the shielded coupled microstrip line will be compared with those from [16] and [17]. Also, influences of different parameters on characteristic impedance and effective dielectric permittivity will be shown. In order to compare some of the HBEM results, the analysed structure will be also modelled using FEMM software [18]. Both modes ("even" and "odd") are supported and analysed.

2 Theoretical Background

A shielded multilayered microwave transmission line with an arbitrary cross-section is shown in Fig. 1. Dielectric layers are assumed to be lossless, isotropic and homogeneous. The HBEM is very suitable to analyse microstrip lines of different configurations, with arbitrary number of conductors and dielectric layers as well as infinitesimally thin or finite metallization thickness. It can be also applied to analyse single and coupled transmission lines. It can be applied if a conductor touches a dielectric interface, straddles a dielectric interface or is a totally within one dielectric media as shown in Fig. 1.

In order to form an equivalent HBEM model, each surface of the conductors as well as the boundary surface between any two dielectric layers is divided into a large number of segments [9]. Each of those segments is replaced by equivalent electrodes (E_{es}), placed at their centres. The corresponding HBEM model for the system from Fig. 1 is shown in Fig. 2.

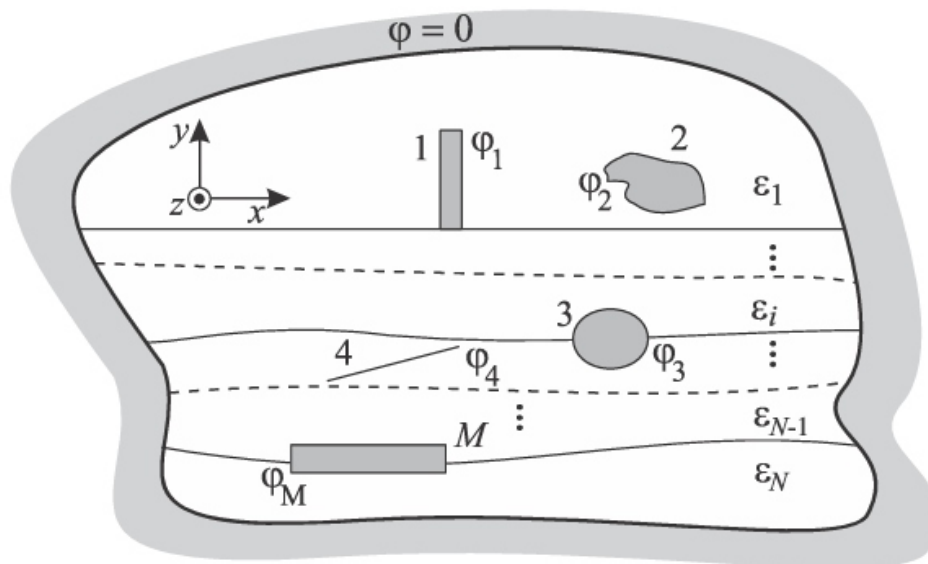


Fig. 1 – *Shielded multilayered microwave transmission line.*

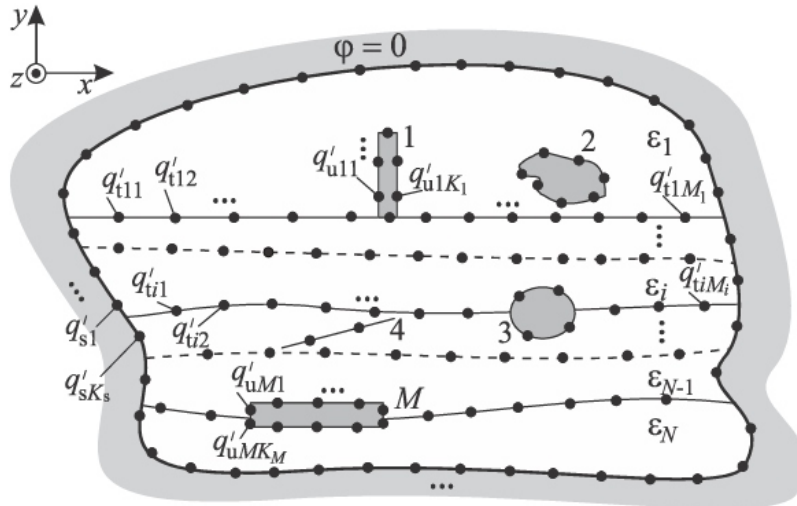


Fig. 2 – HBEM model.

The segments at any boundary surfaces between two layers are replaced by discrete equivalent total charges placed in the air. In Fig. 2 those charges are denoted with q'_{ij} , where $i = 1, \dots, (N - 1)$ and $J = 1, \dots, I_{M_i}$. N is the number of dielectric layers with permittivity ϵ_n ($n = 1, \dots, N$) and $N - 1$ is the number of boundary surfaces between two dielectric layers. Index "t" denotes the total charges. Those charges are equal to the polarized charges, because the free charges at those surfaces do not exist. The free charges exit only at the PEC surfaces.

At the boundary surface between the PEC and the dielectric, the free and polarized charges exist. Their sum gives the total charges. But, the satisfying results are obtain using approximation that polarized charges at that boundary surface can be neglected and only free charges taken into account [8]. Those charges are placed in the corresponding dielectric layer and denoted in Fig. 2 with q'_{uMk} and q'_{sKs} , where q'_{uMk} and q'_{sKs} , where $m = 1, \dots, M$, $k = 1, \dots, K_m$ and $l = 1, \dots, K_s$. M is the number of PECs. Indices "u" and "s" denote charges placed on the PECs and on the shield, respectively.

The type of equivalent electrodes depends on the problem geometry. When the system is plan parallel as those from Fig. 1, the EEs are thin cylindrical electrodes. In the case of 3D problems, spherical electrodes can be used as Ees. For solving 2D problems with axial symmetry, toroidal electrodes are used as Ees.

The potential of the equivalent electrodes placed at the PECs surface is the same as the potential of PECs themselves:

$$\phi_{mk} = \phi_m, \quad k = 1, \dots, K_m, \quad m = 1, \dots, M, \quad (3)$$

where ϕ_{mk} is the potential of k-th EE at m-th PEC and ϕ_m is the potential of m-th PEC, Fig. 2.

Using the Green's function, the electric scalar potential at any point of the system can be defined. The HBEM application has the aim to obtain the quadratic system of linear equations with unknown free charges of PECs, total charges per unit length at boundary surfaces between dielectric layers, and an known additive constant Φ_0 that depends on the chosen referent point for the electric scalar potential. As it is described in detail in [9], using the PMM for the potential of the inner and the outer conductors, the PMM for the normal component of the electric field, and the electrical neutrality condition, it is possible to determine unknown free charges per unit length on conductors, total charges per unit length on the boundary surfaces between layers, and the unknown constant Φ_0 .

A computer code for solving that system and characteristic parameters calculation is developed by authors of this paper.

The HBEM results have been compared with those obtained by FEMM [18]. The results divergence is defined as:

$$\delta[\%] = \frac{|Z_c^{\text{HBEM}} - Z_c^{\text{FEMM}}|}{Z_c^{\text{FEMM}}} \cdot 100. \quad (4)$$

3 Numerical Results

The geometry of shielded symmetrical coupled microstrip line with finite metallization thickness t and three layers with permittivities 1 shown in Fig. 3. ϵ_1, ϵ_2 and ϵ_3 is.

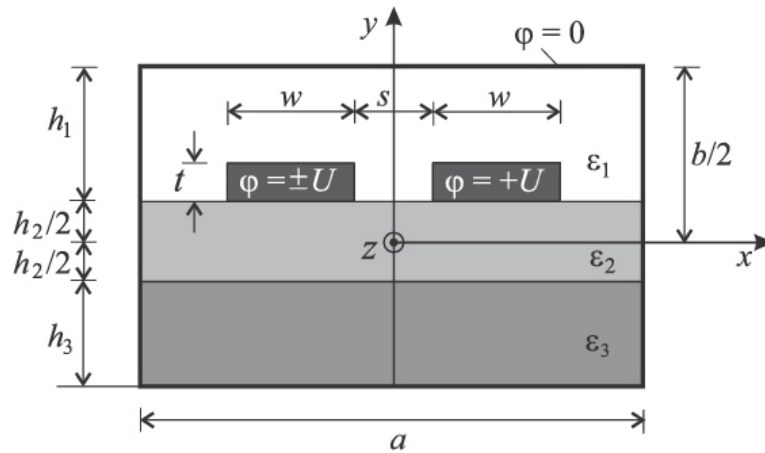


Fig. 3 – Shielded symmetrical coupled multilayered microstrip line.

With w is denoted the width of both inner conductors, s is the distance between the inner conductors, h_1 , h_2 and h_3 are heights of corresponding dielectric layers, a and b are the width and height of the shield, respectively. Some of typical materials which can be used as dielectric layers are mentioned in [19]. Some of them are used in this paper for characteristic parameters calculation. Their permittivities are: $\epsilon_r = 3.78$, $\epsilon_r = 6.1$, $\epsilon_r = 9.35$ and $\epsilon_r = 11.0$.

The convergence of microstrip line characteristic impedance for “even” and “odd” modes is shown in Fig. 4. Dimensions and layers permittivities of microstrip line are:

$$\epsilon_{r1} = \epsilon_{r3} = 1, \quad \epsilon_{r2} = 9.35, \quad a/w = 4.0, \quad s/w = 1.0, \\ t/w = 0.1, \quad h_1/w = h_3/w = 0.8, \quad h_2/w = 0.4.$$

N_{tot} is the total number of unknowns.

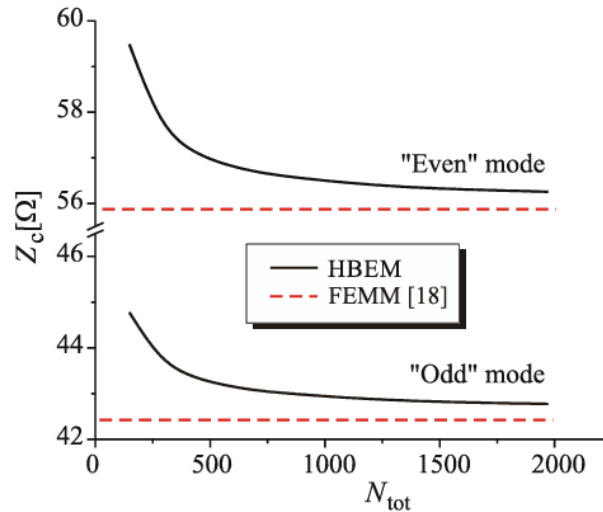


Fig. 4 – Characteristic impedance results convergence for “even” and “odd” modes.

A good convergence of the results is achieved for both modes. The values obtained using FEMM [18] are denoted with dashed lines. In order to verify the accuracy of the HBEM values, the comparison of HBEM and FEMM results for the effective dielectric permittivity and the characteristic impedance versus $3h/w$ is given in Tables 1 and 2.

The microstrip dimensions and layers permittivities are:

$$\varepsilon_{r1} = 1, \varepsilon_{r2} = 6.1, \varepsilon_{r3} = 9.35, a/w = 4.0, b/w = 2.0, s/w = 1.0, \\ t/w = 0.05, h_2/w = 0.2 \text{ and } h_1/w = (b - h_2 - h_3) / w.$$

Table 1 Verification of results for characteristic parameters of shielded coupled microstrip line versus h_3/w (“even” mode).

$\frac{h_3}{w}$	HBEM		FEMM		$\delta[\%]$
	$\varepsilon_r^{\text{eff}}$	$Z_c [\Omega]$	$\varepsilon_r^{\text{eff}}$	$Z_c [\Omega]$	
0.2	4.8751	31.787	4.8971	31.730	0.18
0.4	4.6878	38.780	4.7156	38.662	0.30
0.6	4.4323	43.225	4.4634	43.062	0.38
0.8	4.1446	45.590	4.1779	45.394	0.43
1.0	3.8130	45.972	3.8490	45.745	0.50
1.2	3.4023	44.045	3.4410	43.797	0.57

Table 2 Verification of results for characteristic parameters of shielded coupled microstrip line versus h_3/w (“odd” mode).

$\frac{h_3}{w}$	HBEM		FEMM		$\delta[\%]$
	ϵ_r^{eff}	$Z_c [\Omega]$	ϵ_r^{eff}	$Z_c [\Omega]$	
0.2	4.5736	30.370	4.5955	30.307	0.20
0.4	4.3414	36.041	4.3702	35.913	0.35
0.6	4.1493	39.130	4.1819	38.961	0.43
0.8	3.9903	40.461	4.0251	40.269	0.48
1.0	2.7196	41.096	2.7574	40.821	0.68
1.2	2.5861	36.015	2.6249	35.772	0.68

From those tables is evident that the results divergence is less than 0.7 %. Increasing the height of the third layer, for "even" mode, the effective permittivity decreases and the characteristic impedance increases. In the other case (for "odd" mode) the characteristic impedance first increases than decreases. The effective permittivity decreases in that case. It should be mentioned that, during the FEMM application, the simulation was done twice – one for the case when the shielded line is air-filled (the dielectric layers are replaced by air) and the second case when the dielectric layers are placed as it is shown in Fig. 3. In both cases the capacitance per unit length of the shielded microstrip line was calculated so the characteristic parameters can be determined.

The comparison of the results obtained applying the HBEM with the results reported in the literature is shown in Fig. 5. The characteristic impedance for "even" and "odd" modes as a function of electrode thickness, for different values of parameter s/w , is shown this figure. The results given in [16] and [17] are also presented in the figure as well as the FEMM results [18].

The microstrip parameters are:

$$\epsilon_{r1} = \epsilon_{r3} = 1, \epsilon_{r2} = 4, a/w = 10.0, h_1/w = h_2/w = 1.0, h_3/w = 2.0.$$

Total number of unknowns is about 1500. As it can be seen from this figure, the results agreement is very good.

Increasing the electrode thickness, the characteristic impedance decreases for both modes, Fig. 5. Increasing the distance between conductors in the case when $1.0 sw$, the characteristic impedance decreases for "even" and increases for "odd" mode.

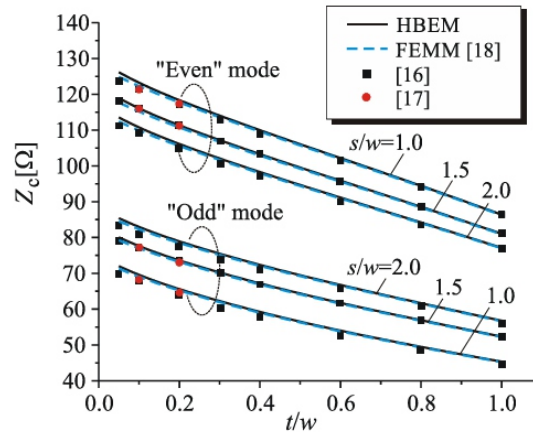


Fig. 5 – Characteristic impedance of shielded coupled microstrip line as a function of electrode thickness.

An influence of layer’s permittivities is also investigated. The characteristic impedance distribution for “even” and “odd” modes for different values of parameter s/w and permittivities ϵ_{r2} and ϵ_{r3} are given in Figs. 6 and 7. The microstrip line dimensions and permittivity of the first layer are: $\epsilon_{r1} = 1$, $a/w = 4.0$, $t/w = 0.05$, $h_1/w = h_3/w = 0.8$ and $h_2/w = 0.4$.

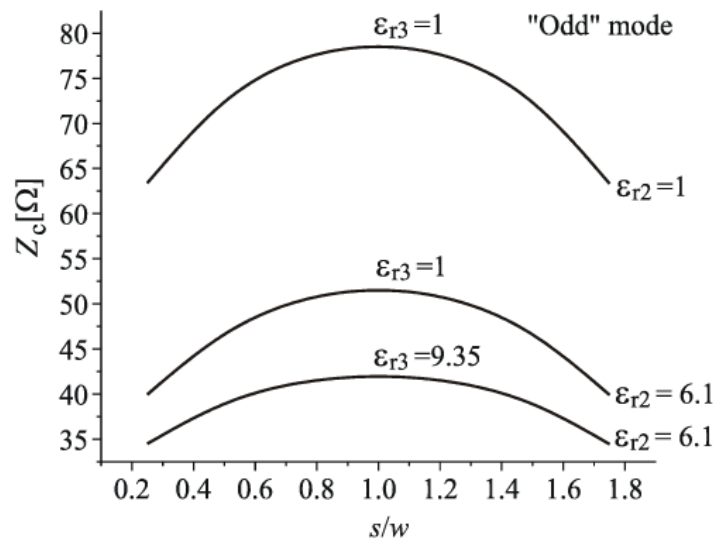


Fig. 6 – Characteristic impedance of shielded coupled microstrip line as a function of distance between conductors and layers permittivities (“odd” mode).

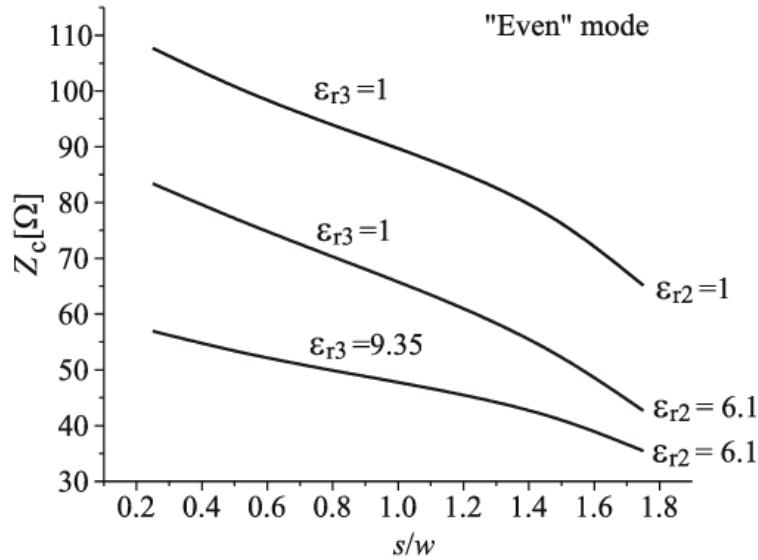


Fig. 7 – Characteristic impedance of shielded coupled microstrip line as a function of distance between conductors and layers permittivities (“even” mode).

The influence of relative permittivities ϵ_{r2} and ϵ_{r3} on the characteristic impedance distribution is evident. The characteristic impedance is greatest when permittivities are equal to 1. Increasing the value of third layer permittivity, when second layer permittivity has constant value, the characteristic impedance decreases for both modes. However, increasing the distance between conductors, the characteristic impedance for “odd” mode first increases than decreases. Such conclusion could not be performed from the Fig. 5. That figure presents results obtain when parameter s/w is 1.0, 1.5 and 2.0. These values are chosen in order to compare the HBEM results with those found in the literature [16, 17]. The characteristic impedance decreases for "even" mode when the distance between the conductors increases.

The second layer height has also the influence on potential distribution. That is shown in Figs. 8 and 9 for “even” and “odd” modes. The potential distribution is given along x-axis. Increasing the second layer height, the conductors distance from the x-axis increases to, so the potential decreases.

The microstrip parameters are:

$$\epsilon_{r1} = \epsilon_{r3} = 1, \epsilon_{r2} = 9.35, s/w = 1.0, t/w = 0.05, h_1/w = h_3/w = (b - h_2) / w.$$

3.1 Computation time

The computation time for different number of unknowns is shown in Fig. 10. The microstrip parameters are:

$$\epsilon_{r1} = \epsilon_{r3} = 1, \epsilon_{r2} = 9.35, a/w = 4.0, s/w = 1.0, \\ t/w = 0.1, h_1/w = h_3/w = 0.8, h_2/w = 0.4.$$

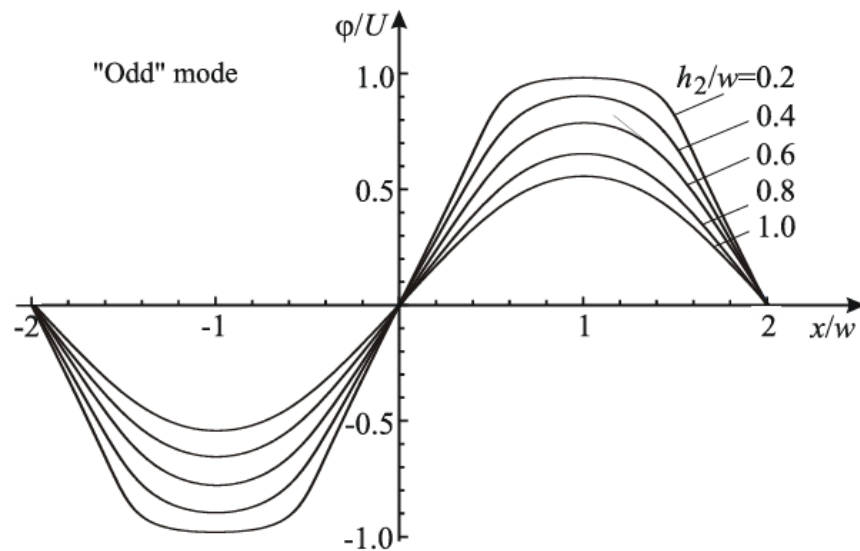


Fig. 8 – Potential distribution along x -axis as a function of second layer height (“odd” mode).

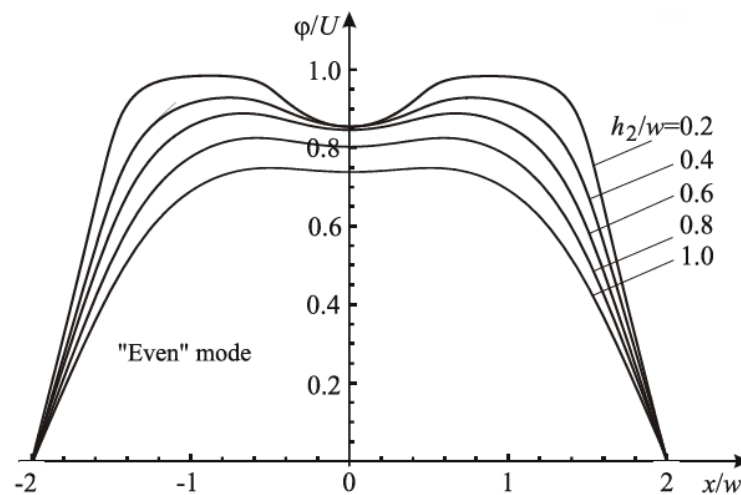


Fig. 9 – Potential distribution along x -axis as a function of second layer height (“even” mode).

Increasing the number of unknowns, the computation time increases too. All calculations were performed on computer with dual core INTEL processor 2.8 GHz and 4 GB of RAM.

The term “computation time” describes the time spent for determining the number of unknowns using an initial number, positioning of the equivalent electrodes, forming the matrix elements, solving the system of equations and the characteristic parameters determination. A computation time distribution is shown in pie chart given in Fig. 11 for tot 1500 N_{tot} . It is evident that the most of the computation time goes to the matrix fill (89% of total computation time).

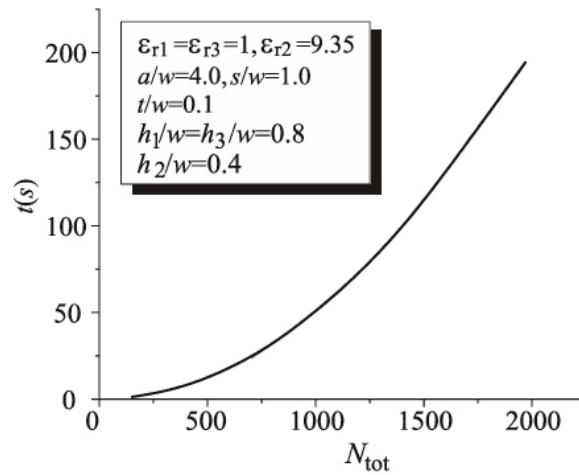


Fig. 10 – Computation time.

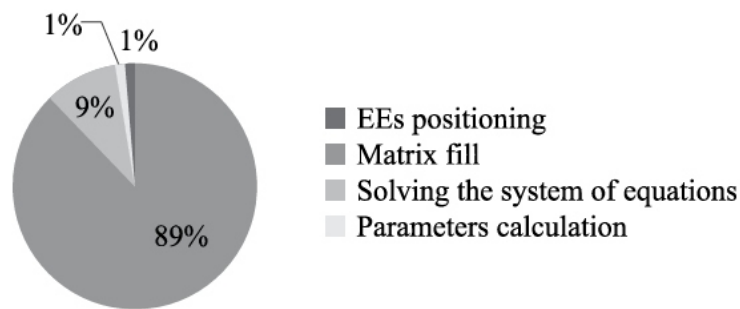


Fig. 11 – Distribution of computation time.

4 Conclusion

An analysis of shielded coupled multilayered microstrip lines has been done using the hybrid boundary element method. The calculation is based on a quasi-static TEM approach. The obtained results show influences of different parameters on microstrip lines characteristic parameters. Those results are verified with the FEMM results and data available in the literature obtained using other methods. Very good results agreement can be noticed. Overall analysis showed that the HBEM is a simple, fast and sufficiently accurate procedure which can be applied to various structures with arbitrary number of dielectric layers and conductors. The finite metallization thickness is also taken into account so the influence of that parameter on characteristic impedance distribution was noticed. The computation time is very short.

5 Acknowledgement

This research was partially supported by funding from the Serbian Ministry of Education and Science in the frame of the project TR 33008.

6 References

- [1] T. Fukuda, T. Sugie, K. Wakino, Y.D. Lin, T. Kitazawa: *Variational Method of Coupled Strip Lines with an Inclined Dielectric Substrate*, Asia Pacific Microwave Conference, Singapore, 07-10 Dec. 2009, pp. 866–869.
- [2] T.G. Bryant, J.A. Weiss: *Parameters of Microstrip Transmission Lines and of Coupled Pairs of Microstrip Lines*, IEEE Transactions on Microwave Theory and Technology, Vol. 16, No. 12, Dec. 1968, pp. 1021–1027.
- [3] T.N. Chang, C.H. Tan: *Analysis of Shielded Microstrip Line with Finite Metallization Thickness by the Boundary Element Method*, IEEE Transactions on Microwave Theory and Technology, Vol. 38, No. 8, Aug. 1990, pp. 1130–1132.
- [4] Z. Pantic, R. Mittra: *Quasi-TEM Analysis of Microwave Transmission Lines by the Finite Element Method*, IEEE Transactions on Microwave Theory and Technology, Vol. 34, No. 11, Nov. 1986, pp. 1096–1103.
- [5] S. Musa, M. Sadiku: *Finite Element Method Analysis of Symmetrical Coupled Microstrip Lines*, International Journal of Computing and Digital Systems, Vol. 3, No. 3, Sept. 2014, pp. 189–195.
- [6] A.Z. Elsherbeni, C.E. Smith, B. Mounneh: *Minimization of the Coupling between a Two Conductor Microstrip Transmission Lines using Finite Difference Method*, Progress in Electromagnetic Research – PIER, No. 12, 1996, pp. 1–35.
- [7] D.M. Velickovic: *TEM Analysis of Transmission Lines using Equivalent Electrodes Method*, 3rd International Conference on Telecommunications in Modern Satellite, Cable and Broadcasting Services – TELSIKS 97, Niš, Serbia, 08-10 Oct. 1997, Vol. 1, pp. 64–74.
- [8] S. Ilić, M. Perić, S. Aleksić, N. Raičević: *Hybrid Boundary Element Method and Quasi TEM Analysis of 2D Transmission Lines - Generalization*, Electromagnetics, Vol. 33, No. 4, April 2013, pp. 292–310.
- [9] M. Perić, S. Ilić, S. Aleksić, N. Raičević: *Application of Hybrid Boundary Element Method to 2D Microstrip Lines Analysis*, International Journal of Applied Electromagnetics and Mechanics, Vol. 42, No. 2, 2013, pp. 179–190.
- [10] S.S. Ilić, M.T. Perić, S.R. Aleksić, N.B. Raičević: *Quasi TEM Analysis of 2D Symmetrically Coupled Strip Lines with Infinite Grounded Plane using HBEM*, XVII International Symposium on Electrical Apparatus and Technologies SIELA 2012, Bourgas, Bulgaria, 28–30 May, 2012, pp. 147–155.
- [11] M. Perić, S. Ilić, S. Aleksić, N. Raičević: *Characteristic Parameters Determination of Different Striplines Configurations using HBEM*, Applied Computational Electromagnetic Society Journal, Vol. 28, No. 9, Sept. 2013, pp. 858–865.
- [12] M. Perić, S. Ilić, S. Aleksić, N. Raičević: *Examples of HBEM application for multilayer problems solving*, International Symposium on Theoretical Electrical Engineering, Pilsen, Czech Republic, 24-26 June 2013, I-31–I-32.
- [13] M. Perić, S.S. Ilić, S.R. Aleksić, N.B. Raičević, A.N. Vučković: *Covered Microstrip Line with Ground Planes of Finite Width*, 11th International Conference on Telecommunications in Modern Satellite, Cable and Broadcasting Services – TELSIKS 2013, Niš, Serbia, 16-19 Oct. 2013, pp. 37–40.
- [14] M. Perić, S. Ilić, S. Aleksić, N. Raičević, M. Bichurin, A. Tatarenko, R. Petrov: *Covered Microstrip Line with Ground Planes of Finite Width*, FACTA Universitatis – Series: Electronics and Energetics, Vol. 27, No. 4, Dec. 2014, pp. 589–600.
- [15] S. Kossłowski, F. Bögelsack, I. Wolff: *The Application of the Point Matching Method to the Analysis of Microstrip Lines with Finite Metallization Thickness*, IEEE Transactions on Microwave Theory and Technology, Vol. 36, No. 8, Aug. 1988, pp. 1265–1271.

-
-
- [16] N.H. Zhu, W. Qiu, E. Y. B. Pun, P. S. Chung: *Quasi-Static Analysis of Shielded Microstrip Transmission Lines with Thick Electrodes*, *IEEE Transactions on Microwave Theory and Technology*, Vol. 45, No. 2, Feb. 1997, pp. 288–291.
- [17] G. Gentili, G. Macchiarella: *Quasi-Static Analysis of Shielded Planar Transmission Lines with Finite Metallization Thickness by a Mixed Spectral-Space Domain Method*, *IEEE Transactions on Microwave Theory and Technology*, Vol. 42, No. 2, Feb. 1994, pp. 249–255.
- [18] D. Meeker, *FEMM4.2*, <http://www.femm.info/wiki/Download>.
- [19] E. Yamashita, K. Atsuki: *Strip Line with Rectangular Outer Conductor and Three Dielectric Layers*, *IEEE Transactions on Microwave Theory and Technology*, Vol. 18, No. 5, May 1970, pp. 238–244.

Analysis of the Impact of Network Architecture on Signal Quality in LTE Technology

Ivana Stojanović^{1,2}, Mladen Koprivica²,
Nenad Stojanović³, Aleksandar Nešković²

ABSTRACT

In this paper, the impact of the network architecture on signal quality in the fourth generation of the public mobile network is analyzed. The analysis was performed using RSRP (Reference Signal Received Power), RSRQ (Reference Signal Received Quality), SINR (Signal to Interference plus Noise Ratio) and throughput parameters in indoor environment. The signal quality parameters were collected by measurement using TEMS Investigation and TEMS Pocket software. The measurements were carried out at the School of Electrical Engineering on the ground floor of the Technical Faculty building for the macro and micro cell scenario. It has been found that better signal quality is ensured in micro cells. Quality of the signal is also considered by the various services provided to the users.

Keywords: LTE, Macro cell, Micro cell, RSRP, RSRQ, SINR, Throughput.

1 Introduction

Mobile radio communications have become a part of everyday life. In the last two decades, mobile communication systems have evolved from an expensive technology that only individuals could afford, to this day when they have become ubiquitous systems used by the majority of the world's population. LTE (Long Term Evolution) technology represents the fourth generation of mobile telecommunication systems. Compared to previous generation's technologies, LTE offers several benefits to operators and users. Improvements in system performance and capacity, better utilization of radio resources and reduced energy consumption are some of the main benefits. One of the main challenges in radio communications is radio network optimization. In the first step, operators plan radio network deploying the base station [1]. After that, network optimization is performed, which requires testing the features on an active mobile network. For this reason, manufacturers of the telecommunication measurement equipment are tasked with finding the simplest way to measure the parameters which are needed for analysis of network performance.

In this paper, an experimental analysis of the performance of LTE technology was performed using an active mobile network on the ground floor building of the School of Electrical Engineering in Belgrade. Services such as web browsing, 32 B packet size ping, media streaming, 800 B packet size ping, file download and file upload were tested. These services represent typical services of LTE technology. In addition, considered services are the most commonly used services by students who spend time in the building of the School of Electrical Engineering. To analyze LTE network performances RSRP (Reference Signal Received Power), RSRQ (Reference Signal Received Quality), SINR (Signal to Interference plus Noise Ratio) and throughput, were used. Macro and micro cells scenarios were considered during measurements. A macro cell scenario is a case when end user equipment is serviced by a macro cell base station, and a micro cell scenario is when a micro cell base station does it. A comparative analysis of the results obtained in macro and micro cells scenarios was performed. All measurements were performed in the indoor environment.

Similar research has been performed within UMTS (Universal Mobile Telecommunication Systems) technology (third generation of public mobile network). In [2] it was shown that by installing the micro

cells at appropriate distances from macro cells, it is possible to improve the functionality of the network. Network enhancement is shown through the achieved throughput, SNR (Signal to Noise Ratio) and the level of the receiving signal as parameter of signal quality in the UMTS network.

The rest of the paper is organized as follows. The second chapter discusses LTE technology, its basics, features and parameters of interest. Chapter three contains a description of used measurement procedure. In chapter four are presented the results of the measurements and a comparative analysis of the obtained results. Discussions on relationship between QoS (Quality of Service) and QoE (Quality of Experience) are given in chapter five. Finally, chapter six concludes the paper.

2 Long Term Evolution

2.1 Basic concepts of LTE technology

LTE is designated as fourth generation of radio technology. The goals of switching to LTE network technology are: providing higher data rate transmission to the end users, improving spectral efficiency, realizing significantly more efficient packet switching, improving and increasing the number of services and their implementation, translating the mobile network to a only packet network and better integration with existing standards of signal processing and transmission [3].

On the downlink, LTE uses an OFDMA (Orthogonal Frequency Division Multiple Access) multiple access system, which gives system that is more robust with increased capacity. Increasing the capacity of a telecommunication channel is achieved by multiplexing users' low rate data across channel with wide bandwidth, while robustness is achieved by allocating user traffic by frequency to avoid narrowband interference and multiple propagation fading. On the uplink it is used the SC-FDMA (Single Carrier - Frequency Division Multiple Access) multiple access system, which is the most important factor energy efficiency, to increase coverage and reduce user equipment cost and energy consumption. SC-FDMA has a low PAPR (Peak to Average Power Ratio) which is the main reason for using this technique on the upload communication side [4].

This approach, which is based on using two different systems on the downlink and uplink, ensures orthogonality among users, reducing interference and improving network capacity [4]. Depending on the available spectrum, the bandwidth can be selected in the interval from 1.4 MHz to 20 MHz. The 20 MHz bandwidth provides up to 150 Mb/s throughput on the downlink when is used 2x2 MIMO (Multiple Input Multiple Output) and up to 300 Mb/s when is used 4x4 MIMO system. Uplink data rates transmissions can reach up to 75 Mb/s.

2.2 Signal quality parameters of LTE technology

BER (Bit Error Rate) is the most commonly used parameter for evaluation of the performance of digital telecommunication systems. Some other parameters are used for assessing signal quality in some specific telecommunication systems to provide the best possible service to users. RSRP, RSRQ and SINR are signal quality indicators that are often used in optimization of the public mobile network of LTE technology. RSRP represents the level of signal strength at the receiving side but does not show signal quality but it is an indicator of cell coverage [5]. The RSRP values are expressed in dBm and it is used as a metric for reselection and handover decision.

RSRQ is the parameter that indicates the quality of the received signal [5]. To get the final value of RSRQ, in the first, total signal (useful signal, interference and noise), which is received in one OFDM (Orthogonal Frequency Division Multiplex) symbol is measured, thereby is obtained the RSSI (Received Strength Signal Indicator) value. In parallel, the RSRP parameter

value is also measured. The relation of these two parameters multiplied by the number of resource blocks gives a final value of RSRQ, which can be represented by the equation:

$$RSRQ = \frac{RSRP}{RSSI} N_{RB}, \quad (1)$$

where N_{RB} represents the number of resource blocks that depend on the bandwidth used in LTE technology. SINR is the quality parameter that is measured by the user equipment, allowing the choice of the most appropriate modulation and coding scheme for the data transmission. Each resource block calculates SINR and user equipment converts obtained values to CQI (Channel Quality Indicator). After conversion, CQI values are being sent to the base station [6].

If the user is located in a rural area, only the RSRP level of signal is observed due to the small number of base stations, which are covering the area. However, if the user is in an urban area with a good level of RSRP, but there is a high interference due to the existence of several base stations in that area, a decision when is necessary that the user terminal served by another base station (make handover) or remain connected on the one that currently serving it, can be made based on level of RSRQ [7].

Throughput represents the bit rate per unit of time in digital telecommunication systems. Data rate transmission directly affects the performance of the public mobile network, and especially on the QoS based on packet switching [8].

3 Measurements

Measuring equipment consisted of laptop computer with TEMS Investigation software installed on it and mobile device Sony Xperia Z3 D6603 with TEMS Pocket software installed on user equipment. TEMS Investigation is a powerful software tool for optimization, verification, solving problems and maintaining public mobile networks. It collects and processes data from which performs real-time analysis. Software tool supports technologies like LTE (Frequency Division Duplex, FDD and Time Division Duplex, TDD), WCDMA (Wideband Code Division Multiple Access) / HSPA (High Speed Packet Access) / HSPA+, GSM (Global System for Mobile Communication) / GPRS (General Packet Radio Services, Wi-Fi (Wireless-Fidelity), etc. The measurement procedure was performed at the ground floor of building of School of Electrical Engineering, University of Belgrade, for the macro and micro cell scenarios. Measurements were made during the working day due to the highest network load during that period. Telekom Srbija's mobile network was used to test LTE technology services. All measurements were made in an indoor environment. For testing purpose, a script was prepared within the TEMS software. The script consisted of several services running in the following order: 32 B packet size ping of google.com, blic.rs web browsing, 32 B packet size ping of private IP address, data download for 10 seconds, data upload for 10 seconds, google.rs web browsing, 3 MB size of data download, 1 MB size of data upload, YouTube web browsing, 800 B packet size ping of private IP address and streaming media from the YouTube. These services are usually used during the network drive test. As soon as one service was completed and the measurement of it was finished, another service was automatically started. It was taken a little more than three minutes to measure all of the parameters and services. In order to cover the entire hallway of the ground floor of the School of Electrical Engineering, it was necessary to repeat the script three times, so the measurement time was about nine and a half minutes.

Looking at Fig. 1, the starting point of the measurement was the right bottom corner of the hall (red circle). The measurement was continued by moving along the longer part of the hall to the left, then up

and right to the middle of the up part of the hall (red arrows). In the central part of the hall was made a circle (blue arrows). After that circle, and returning to the middle of the upper part of the hall, the movement continued to the right up corner and finally, the movement was completed at the starting point (orange arrows). This way, the entire hall was covered.

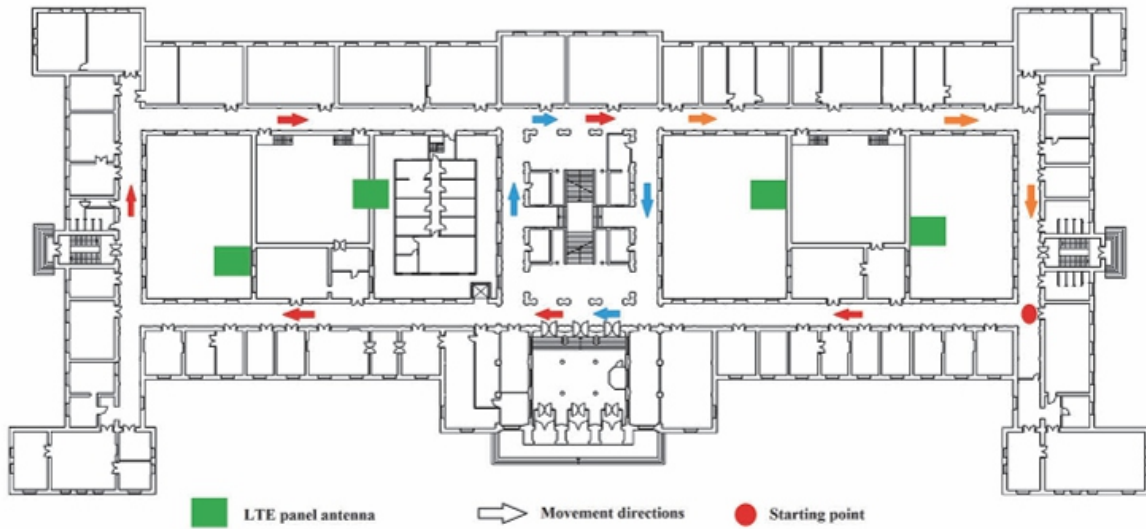


Fig. 1 – Ground floor scheme of the School of Electrical Engineering with LTE technology base stations antenna layout.

The location of the base stations antenna and the layout of the ground floor where measurements were performed are shown in Fig. 1. The positions of the LTE panel antennas are marked with green color.

4 Results

Obtained results are presented graphically, calculating CDF (Cumulative Distribution Function), similar as in [9], where the measurement was performed in outdoor environment. The range of referent values of RSRP, RSRQ and SINR parameters are shown in the Table 1. These parameters determine level of signal quality, that is, QoS provided to the user.

Table 1. Signal level values versus signal quality.

	Parameters	RSRP [dBm]	RSRQ [dB]	SINR [dB]
Signal quality	Excellent	> -84	> -5	> 12.5
	Good	-102 to -85	-11 to -6	10 to 12.5
	Fair	-111 to -103		7 to 10
	Poor	< -112	< -12	< 7

Level of RSRP for macro and micro cell scenarios is shown on Fig. 2a. Values of RSRP are in range from -120 dBm to -95 dBm for a macro cell scenario, so the values of signal include three levels from the Table 1, with poorer signal quality. About 25% of the measured signal values have poor quality, 70% have fair quality, while the remaining 5% have satisfactory signal quality. RSRP signal values are in

range from -90 dBm to -55 dBm for micro cell scenario, which is excellent level of the signal based on data from Table 1. It can be concluded that the signal level is significantly better in the case of a micro cell scenario, which is expected, since the micro base station is located on the wall of the School of Electrical Engineering, so it provides better signal coverage.

Values in range from -11 dB to -6 dB represent good signal quality for RSRQ parameter. For the macro cell scenario, RSRQ has values from -20 dB to -5 dB, while for the micro scenario the RSRQ values are in range from -16 dB to -2 dB, which is shown on Fig. 2b. It can be seen that the level of RSRQ is better in the micro cell scenario as it expected due to the proximity of the micro base station to the user. In addition, both scenarios include all three signal quality levels presented in Table 1, with very few values of excellent signal quality.

Obtained results of SINR parameter are illustrated in Fig. 2c. As RSRP and RSRQ, SINR also has much better values of signal in micro cell scenario.

About 60% of all measured SINR values in macro cell scenario and only 2% in micro cell scenario have poor signal quality. A very high signal quality in micro cell scenario is shown with the 92% of all measured signals with values over 12.5 dB. In addition, in macro cell scenario, only the 6% of all measured values have signal with excellent quality.

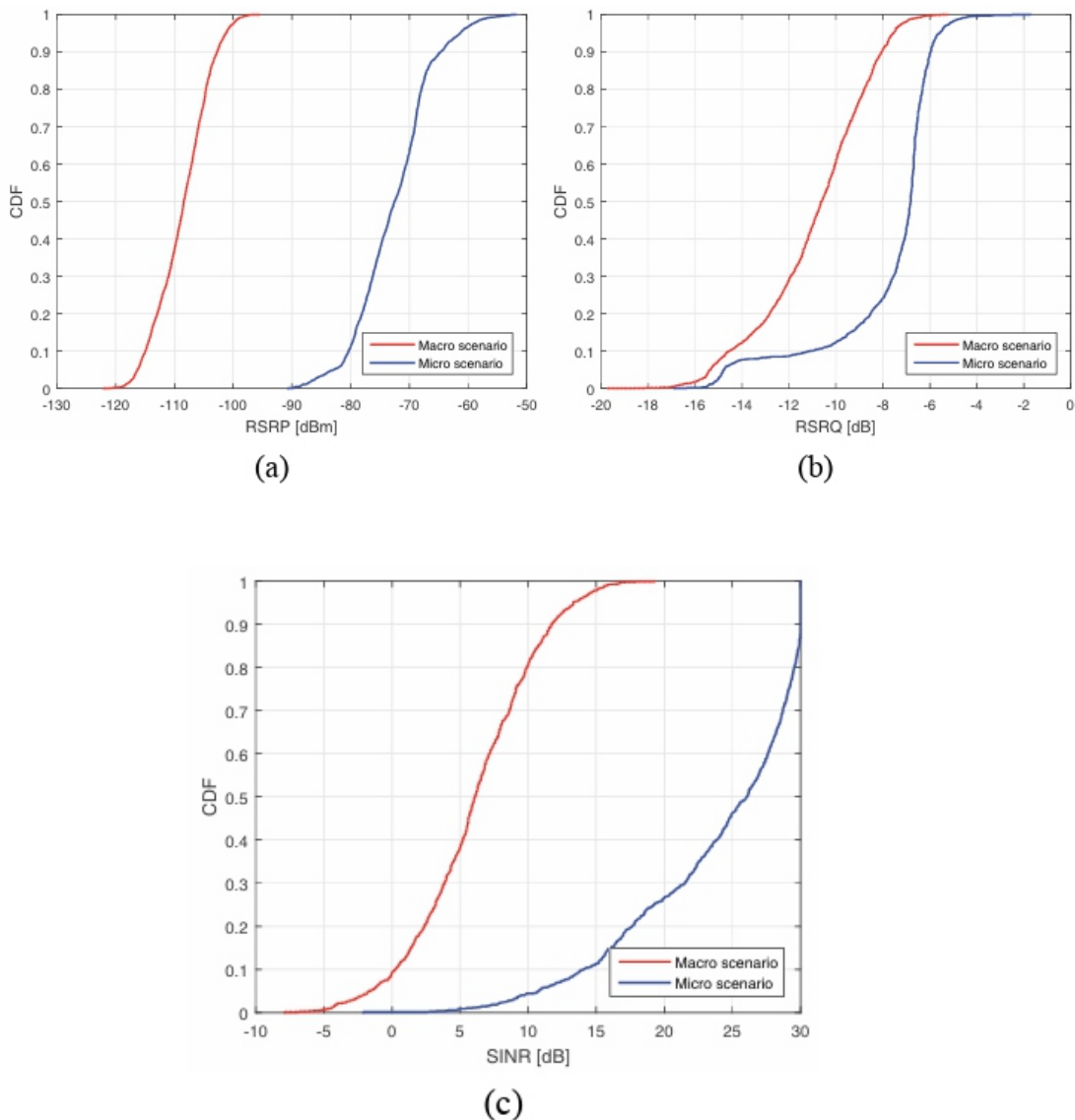


Fig. 2 – Comparison of the CDF for the macro and micro cell scenario of (a) RSRP values; (b) RSRQ values; (c) SINR values.

Results of throughput comparison for the two analyzed scenarios are shown on Fig. 3, where are illustrated downlink and uplink data transmissions using CDF. Fig. 3a presents normalized downlink throughput for the 10 seconds of data download service. Normalization is performed by dividing each throughput values by maximum measured value for the 10 seconds download service when the user equipment was served by micro cell. Higher throughput is achieved in the case of micro cell scenario compared to the macro cell scenario by about twice the value.

In the case of uplink data transmission for the 10 seconds duration data upload service, higher throughput values were achieved in micro cell scenario. The difference in the transmission rates between macro cell and micro cell scenarios is slightly smaller than in the case of downlink transmission. In this case, also, the values of throughput are normalized by maximum value of uplink throughput during 10 seconds data upload in the micro cell scenario. Fig. 3b shows the uplink throughput in macro cell and micro cell scenarios.

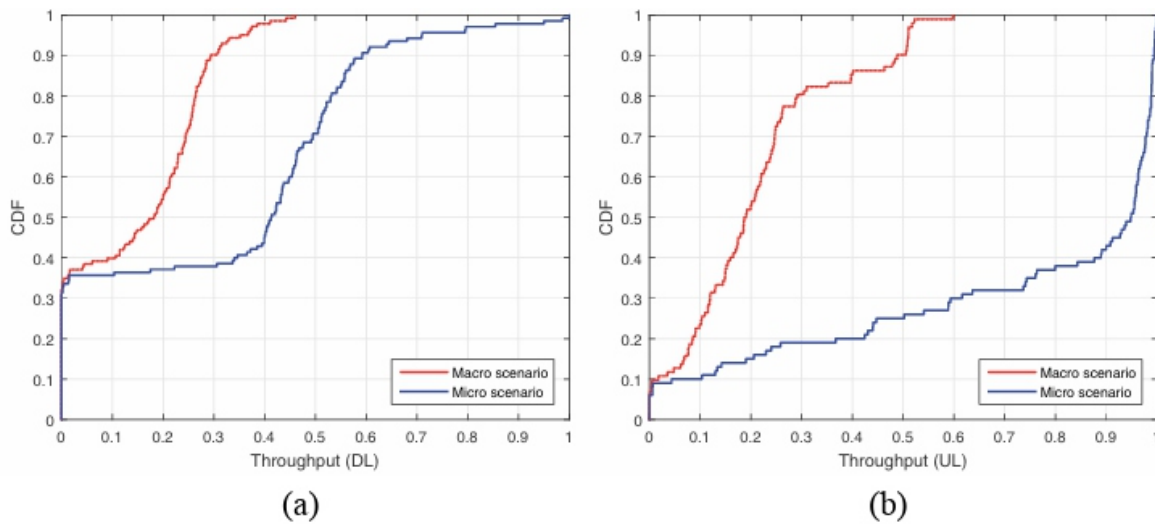


Fig. 3 – Throughput during 10 seconds for macro and micro cell scenario in case of (a) Download; (b) Upload.

Fig. 4 presents signal quality in the form of RSRQ, RSRP and SINR in relation to the most common services provided to the users. The results are obtained after averaging the signal level after each of the three repetitions of the script during the measurement and the three new obtained values are averaged again. This is repeated for each service separately. Analyses are performed for data download for 10 seconds, data upload for 10 seconds, download 3 MB data, upload 1 MB data, loading YouTube and streaming media from YouTube. These services are selected because they are the most commonly used of all the measured services during the research. Required time to download 3 MB of data is significantly shorter than data download for 10 seconds because LTE technology provides very high rate of data transmission. The same goes for upload service.

The RSRP values in macro cell scenario indicate that for all services, the signal is at the border of fair quality, which significantly affects the communication performance. In addition, in the macro scenario, for most tested services, the RSRQ parameter has values around the boundary between fair (good) and poor. Poor signal quality occurs during 10 seconds data download, while for loading YouTube the signal

was slightly better quality than the level of signals of other services. Similar results were obtained with the SINR parameter. All tested services have a poor level of signal quality except YouTube browsing where signal has a fair quality.

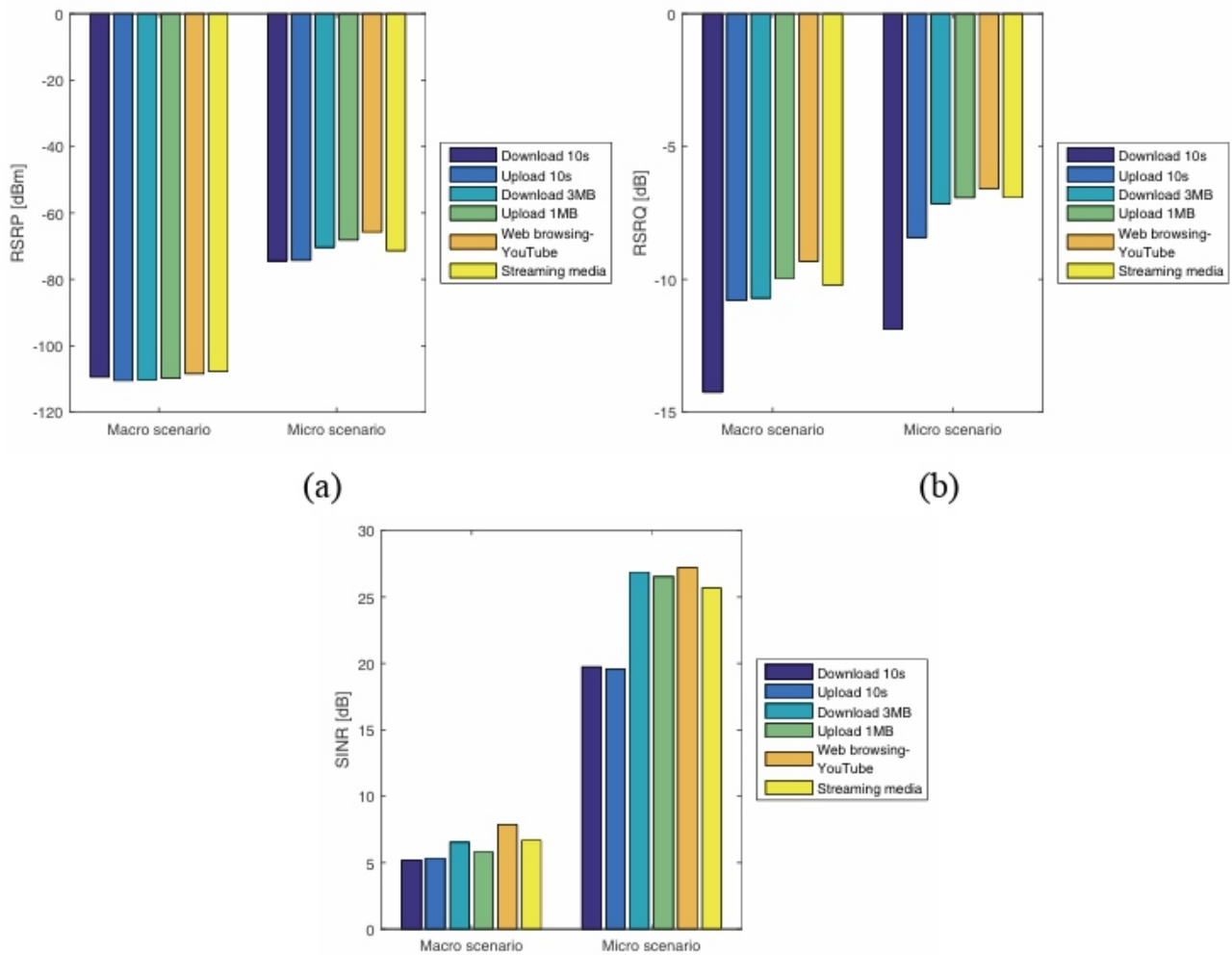


Fig. 4 – Average values for the macro and micro cell scenario for different services in case of (a) RSRP; (b) RSRQ; © SINR.

Different results were obtained in micro scenario. Observation of the RSRP parameter revealed a very high level of signal quality for all tested services. All values of RSRP parameter showed that is achieved an excellent level of signal when the micro cell base station serves the user equipment. The RSRQ parameter also gives slightly different results in scenario of micro cell. The data download during 10 seconds has poor level of signal, while all other services can be classified as signal with good quality when the values obtained from the measurement are compared with the values in Table 1. Values of SINR for all tested services are very high, so all have the excellent signal quality. Two services, data download and data upload during 10 seconds, have lower values than the other four, but still are about 7 dB higher than the border value of 12.5 dB.

Fig. 5 shows the RSRP and RSRQ levels of signal measured along the hallways of the School of Electrical Engineering in the micro cell scenario. Fig. 5a shows values of RSRP parameter. Based on the obtained results, it can be observed that the signal quality was extremely high all the time, so, it can be said that there is not any signal degradation occur.



(a)



(b)

Fig. 5 – (a) Level of RSRP; (b) Level of RSRQ; in micro cell scenario during the movement through the hall of School of Electrical Engineering.

Values of RSRQ parameter are shown on the Fig. 5b. In this case, in some spots, there was some degradation of the signal to the poor level, according to Table 1. These points are colored in yellow and represent range values from -19 dB to -14 dB. It is important to emphasize here that during the movement through the hallway and the measurements, eight handovers occurred between the four cells of micro base stations whose locations are shown in Fig. 1 and marked with the small hands.



(a)



(b)

Fig. 6 – (a) Level of RSRP; (b) Level of RSRQ; in macro cell scenario during the movement through the hall of School of Electrical Engineering.

Fig. 6 illustrates the RSRP and RSRQ levels of signal in the macro cell scenario. Fig. 6a shows values of RSRP in the hall of the School of Electrical Engineering. There can be seen that there are not the values of signal with excellent quality. It can be said that most of measured signals have fair signal quality (orange points). There are, on some spots, signals with good (yellow points) and poor (red points) quality. The RSRQ parameter shows, on the Fig. 6b, that the most signal values have good (fair) quality (light green points). Some spots have better or worse signal, but same as RSRP, and RSRQ parameter gave the worse results in relation to micro cell scenario. In this case, it came to 18 handovers. It can be explained by the fact that the some macro base stations have the same coverage area. Also, micro base stations have better indoor environment coverage, so provide better service.

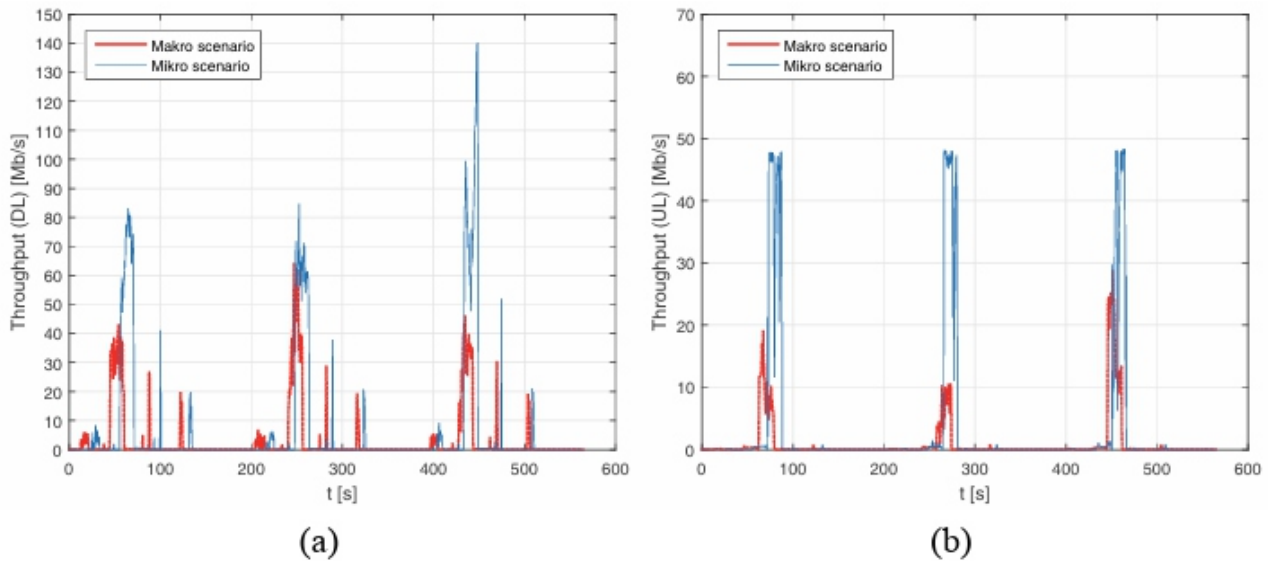


Fig. 7 – (a) Downlink; (b) Uplink; throughput values during the measurement.

The values of throughput during the measurement on downlink and uplink in micro cell and macro cell scenarios are shown on Fig. 7. From the graphics, intervals in which three scripts were repeated can be seen. Fig. 7a shows the measurements obtained on the downlink, where can be seen that the data rate transmissions were significantly higher in micro cell scenario. That difference is greatest with the third repetition of the script, for 90 Mbps, within the data download service during 10 seconds. For other services, the differences in data rate transmissions for macro and micro scenarios are minimal. The maximum data rate transmission is achieved in micro cell scenario and its value is 140 Mbps.

The similar results are obtained on the uplink. The data rate transmissions were significantly higher within micro cell scenario when running all three scripts and the biggest difference was in the second repetition, where difference was about 40 Mbps. The maximum achieved data rate transmission was about 50 Mbps in the micro cell scenario. In the macro cell scenario, a maximum data rate transmission of 30 Mbps was achieved. Based on the obtained results, it can be concluded that 2×2 MIMO systems are used at the measuring location. In order to meet the needs of the users, it is necessary to ensure consistency at high data rates, especially at downlink (over 100 Mbps at any time).

5 QoE in radio network optimisation

The main goal of all operators is to provide the best possible service to the users. For this reason, during optimisation of public mobile network, it is necessary to take into account subjective quality assessments by users for different kinds of services. However, collecting subjective quality assessments can be long, tedious and expensive. As a consequence, operators are changing legacy network management approaches, focused on network performance and QoS to a more modern approach focused on user opinion and quality of experience QoE [10]. Good network QoS parameters do not necessarily mean that the end user is satisfied with the provided service, since his satisfaction depends on other factors. Thus, in order to measure the user satisfaction, it needs to define the QoE, which takes into account factors like expectation, requirements and perception of the user, content type provided by the service, user's device features, network QoS and the context in which the user is using the service, like the access type, movement and location [11].

Different models have been developed so far to map QoS to QoE. For example, mapping models for web browsing [11] and video transmission in wireless communications [12] are presented. The QoE data for

the web browsing model was determined by applying a model that predicts the perceived quality for this type of service through the web page download time. The model was developed using machine learning techniques, more specifically the SVR (Support Vectors Regression) algorithm. The models take as input QoS metrics that can be measured, for instance, in drive tests. The models map these metrics in a single metric of QoE, the MOS (Mean Opinion Score) [11]. In [12], video dataset with network QoS parameters such as packet loss rate, jitter, delay and bandwidth are presented. The video dataset contain subjective assessments that can be helpful to create QoS to QoE mapping model for special radio network service - video transmission. Nowadays, radio network services such as live streaming video using YouTube or Facebook depends a lot on subjective perception [10]. The great challenge for all researcher is to create optimal and universal model for QoS to QoE mapping for all services which operators provide. After creation and testing, implementation of mapping models will significantly improve the network performance.

In addition, some QoS to QoE mapping models can be used to define decision to perform handover and improve it [13]. Existing handover algorithms consider radio (signal strength...) or QoS as context parameters for handover decisions, so there is plenty of space for improvement.

6 Conclusion

The impact of network architecture on the signal quality of the LTE communication system is presented in this paper. Through measured values of RSRP, RSRQ and SINR parameters, it is shown that better signal quality is obtained for the micro cell scenario. In throughput analysis, it has been shown that even during download and upload communication, higher throughput is achieved within micro cell scenario, where the data rate transmissions are significantly higher than in the macro cell scenario. In the case of observing the tested services, the worst signal quality occurs during the 10 s data download, while the best quality is achieved loading YouTube. Due to the different coverage areas in the micro cell and macro cell scenario, the number of handovers in the macro cell scenario was more than twice as high as in the micro cell scenario.

Based on obtained results, further implementation of micro cell can improve the area coverage, signal quality. Different radio range and network characteristics in micro cells increase the transmission rate, while decrease traffic on the macro cells. Implementation of femto cell and pico cell can further improve the signal quality, transmission capacity and area coverage in urban environment, especially in indoor environment.

In the further work, it is possible to observe other services as well as other locations where measurements would be made. Also, measurements can be taken over several days to identify some regularities according to the number of users located at the observed location. Traffic in LTE technology is expected to increase in the Republic of Serbia, as implementation of this technology is still ongoing, so it is expected that different results may be obtained. It should be noted that preparations for the implementation of VoLTE (Voice over LTE) technology that will provide voice service, and this service, which is the least resistant to any interference with the wireless telecommunication channel, should be considered by some further analysis. Finally, it would expect more frequent implementation of QoE in the optimization of the public mobile network.

7 Acknowledgments

This paper is an extended version of the work published under the same name (in Serbian) at the 63rd annual meeting ETRAN (Silver Lake, Serbia, June 3-6, 2019), and which was awarded as The Best Young Researcher's Paper at the Telecommunication section.

8 References

- [1] I. R. Maravić, A. N. Nešković: *LTE Network Radio Planning*, *Telfor Journal*, Vol. 4, No. 1, 2012, pp. 26 – 30.
- [2] D. Pouhè, D. Emini, M. Salbaum: *The Use of Microcells as a Means of Optimizing UMTS Networks*, *Proceedings of the Wave Propagation and Scattering in Communication, Microwave Systems and Navigation (WFMN07)*, Chemnitz, Germany, July 2007, pp. 127 – 132.
- [3] B. Krenik: *4G Wireless Technology: When Will It Happen? What Does It Offer?*, *Proceedings of the IEEE Asian Solid-State Circuits Conference*, Fukuoka, Japan, November 2008, pp. 141 – 144.
- [4] H. Holma, A. Toskala: *LTE for UMTS: Evolution to LTE-Advanced*, 2nd edition, John Wiley & Sons, Chichester, UK, 2011.
- [5] F. Afroz, R. Subramanian, R. Heidary, K. Sandrasegaran, S. Ahmed: *SINR, RSRP, RSSI and RSRQ Measurements in Long Term Evolution Networks*, *International Journal of Wireless & Mobile Networks*, Vol. 7, No. 4, August 2015, pp. 113 – 123.
- [6] I. Angri, A. Najid, M. Mahfoudi: *Available Bandwidth and RSRP Based Handover Algorithm for LTE/LTE-Advanced Networks Tested in LTE-Sim Simulator*, *International Journal of Electronics and Telecommunications*, Vol. 65, No. 1, January 2019, pp. 85 – 93.
- [7] D. Aziz, R. Sigle: *Improvement of LTE Handover Performance through Interference Coordination*, *Proceedings of the VTC Spring 2009 – IEEE 69th Vehicular Technology Conference*, Barcelona, Spain, April 2009, pp. 1 – 5.
- [8] Đ. Lukić, M. Koprivica, N. Nešković, A. Nešković: *Experimental Performance Analysis of the 2G/3G/4G Public Mobile Network*, *Proceedings of the 24th Telecommunications Forum (TELFOR)*, Belgrade, Serbia, November 2016, pp. 238 – 241.
- [9] T. Mazloum, S. Aerts, W. Joseph, J. Wiart: *RF-EMF Exposure Induced by Mobile Phones Operating in LTE Small Cells in Two Different Urban Cities*, *Annals of Telecommunications*, Vol. 74, No. 1-2, February 2019, pp. 35 – 42.
- [10] L. R. Jimenez, M. Solera, M. Toril: *A Network-Layer QoE Model for YouTube Live in Wireless Networks*, *IEEE Access*, Vol. 7, May 2019, pp. 70237 – 70252.
- [11] V. C. da Silva Pedras: *Identifying Quality of Experience (QoE) in 3G/4G Radio Networks Based on Quality of Service (QoS) Metrics*, MSc Thesis, Técnico Lisboa, Lisboa, Portugal, 2017.
- [12] F. Battisti, M. Carli, P. Paudyal: *QoS to QoE Mapping Model for Wired/Wireless Video Communication*, *Proceedings of the Euro Med Telco Conference (EMTC)*, Naples, Italy, November 2014, pp. 1 – 6.
- [13] I. Medeiros, L. Pacheco, D. Rosário, C. Both, J. Nobre, E. Cerqueira, L. Granville: *Quality of Experience and Quality of Service-Aware Handover for Video Transmission in Heterogeneous Networks*, *International Journal of Network Management*, No. e2064, February 2019, pp. 1 – 16.

Modified Design of Microstrip Patch Antenna for UWB Applications

Bashar Bahaa Qas Elias¹, Haider Aljanabi²

ABSTRACT

Ultra-wideband (UWB) patch antenna for Ku/K band applications is presented. In this paper, a microstrip line feed has been modified to an elliptical gradient structure, and the conventional radiator patch has been developed through the use of the symmetrically circular slots. These modifications have been used to improve the performance of the antenna significantly. Upper and lower frequency ranges achieve UWB antenna performances start from 11.57 GHz to 21.45 GHz. Proposed antenna exhibits good impedance matching, which makes it convenient to work in various applications. Besides that, the reflection coefficient is reduced attained to -31.81 dB over the operating band. The antenna is developed and analyzed using the commercially available software FEKO simulator based on the method of moments (MoM). Other parameters results such as sidelobe level (SLL) and beamwidth (half power 3 dB) are added and discussed significantly. The proposed design is fabricated and tested experimentally, and the results show that a satisfying agreement with the simulation results.

Keywords: Modified antenna, Ultra-wideband (UWB), Reflection coefficient, Slots, Feed line, FEKO.

1 Introduction

The development of ultra-wideband antennas with high impedance matching, compact size, stable radiation patterns, and low manufacturing costs has attracted lots of attention in recent years [1]. Microstrip patch antennas have been widespread, depending on their low profile, lightweight, ease of fabrication, and compatibility with integrated circuits [2 – 4]. As in the rest of the antennas, they are also given some hindrances, ranging from narrow bandwidth to low gain. Therefore, this paper is mainly concentrated on the bandwidth enhancement procedure. Numerous techniques have been clarified in the past to obtain UWB, performance such as the use of a thick substrate, stacked patches, use of active and passive devices, shorting pins, using an impedance matching network, and different feeding arrangement [5]. Recently, various methods reported in improving the functioning of the impedance bandwidth of the microstrip antenna. This work contains the effect by inserting slots on the radiating structure [6 – 10] and feed reconfiguration. Wireless technology is part of the significant areas of research in the world of communication systems today, and a study of communication systems is incomplete without an understanding of the operation of antennas. These requirements force antenna designers to investigate low profile antennas with an appropriate bandwidth for each band [11 – 14]. Microstrip patch antenna comprises of a radiating patch on one side and ground plane on the other side and a substrate layer as a sandwich between them. To achieve the UWB performance of the microstrip antenna, many researchers and scientists have been publishing more articles in this field. In 2016, Sayed Ali and Deepak Jhanwar designed a compact triple bandnotch direct-fed Flower-shaped Hexagonal Microstrip Patch Antenna for embedding in UWB (Ultra-WideBand) systems [15]. Karmugil and Anusudha proposed an efficient design of a circular shaped microstrip patch antenna for Ultra-Wideband (UWB) applications with partial ground structure [16]. Mewara, Kumawat, and Sharma presented an ultra-wideband antenna consisting of an extra radiating patch with bandwidth enhancement and band notch characteristic [17].

In 2017, Aishvaryaa et al. designed two ultra-wideband frequency reconfigurable microstrip patch antennas for cognitive radio applications, consist of a rectangular patch with microstrip feed - line, and a partial ground plane [18]. Angana et al. proposed a compact microstrip fed band-notched UWB patch antenna with band rejection features to eliminate interference as a result of existing neighboring communication systems within the ultrawideband (UWB) frequency band [19]. Feng and Jin presented a broadband cavity-backed microstrip phased array antenna. The array antenna uses novel single layer cavity-backed microstrip patch elements supporting broad operating frequency band [20]. Antenna designs are simulated and analyzed by FEKO simulator software based on the method of moments (MOM).

2 Antenna Design

The proposed antenna has been designed using the dry wood sheet as a substrate. It has a dielectric constant of 1.4 and a thickness of 7mm. The modified design is implemented in two successive steps. In the first step, the microstrip line employed to feed the antenna has changed to elliptical gradient structures instead of the traditional rectangular line feed. Feed width is gradually decreased in four levels (S4, S3, S2, and S1 respectively) starting from the port of excitation to the edge of the patch. Next, four symmetrical circular slots with a radius of (R) have been drilled into the radiator patch plane with a small triangular patch in each slot. Besides, four semi-circular shapes are placed between them and also subtracted from the patch (see Fig. 1). All the dimensions detailed are illustrated (Table 1).

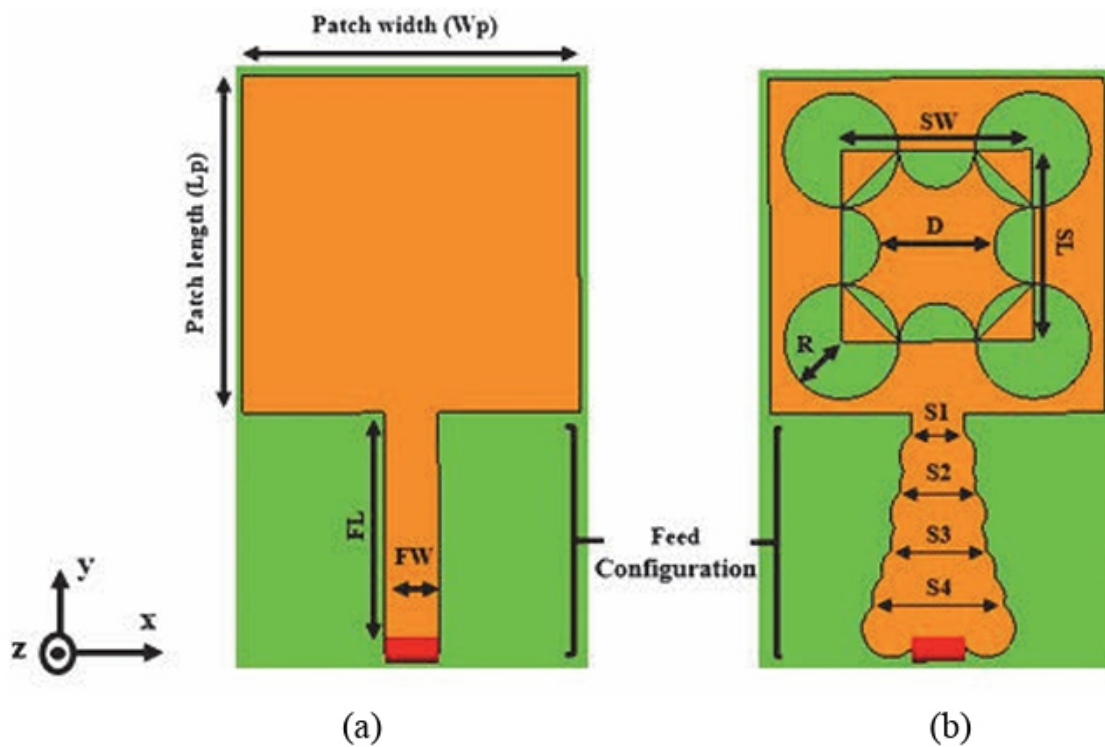


Fig. 1 – Proposed microstrip antenna in x- y plane: (a) conventional antenna; (b) modified antenna.

Table 1 Antenna design parameters.

Parameter	Value
Patch length (L_p)	35 mm
Patch width (W_p)	35 mm
Substrate thickness	7 mm
Dielectric constant	1.4
Feed length (FL)	25 mm
Feed width (FW)	5.61 mm
R	6 mm
D	12 mm
SW	20 mm
SL	20 mm
S1	5.61 mm
S2	7.84 mm
S3	9.84 mm
S4	13.84 mm

3 Simulated Results

The design of the traditional microstrip antenna has been enhanced to reduce the size of the antenna and increase bandwidth. FEKO software based on MoM is used as a simulation tool to analyze the antenna. The results are obtained; the reflection coefficient of the proposed antenna decreased from -11.6 to -31.81 dB at the resonant frequency. Besides that, the relative bandwidth is enhanced to 9880 MHz with the upper and lower frequencies of 21.45 and 11.57 GHz, respectively as compared with its value in the conventional antenna (Fig. 2). The reflection coefficient and bandwidth results are tabulated (Table 2).

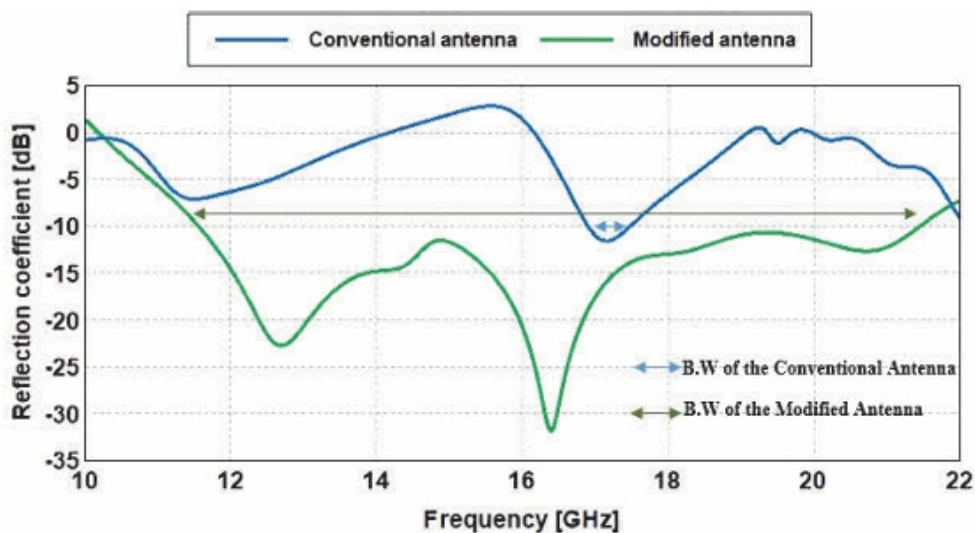


Fig. 2 – Reflection coefficient results of conventional and modified antennas.

Table 2 Reflection coefficient and bandwidth results.

Antenna	Resonant frequency (GHz)	Reflection coefficient (dB)	Upper frequency (GHz)	Lower frequency (GHz)	BW (MHz)
Conventional	17.16	-11.6	17.47	16.92	550
Modified	16.4	-31.81	21.45	11.57	9880

The proposed antenna is used for Ka and K band applications such as satellite communication and radar applications. Total gain characteristics in 3D plots are represented (Fig. 3). It observed that the gain is reduced to half (10 dB) in the proposed antenna (Fig. 3b). On the other hand, this value increases to 15 dB in the upper and lower frequencies of the modified antenna (Figs. 3e and 3f). Besides, the gain is prescribed in polar plots (Fig. 4). It's noted that no back radiation in the proposed antenna, that's will be increasing the radiation efficiency of the antenna. In spite of reduced the gain in a proposed antenna, its value is still acceptable and suitable for use in various applications operates under the given band in this paper.

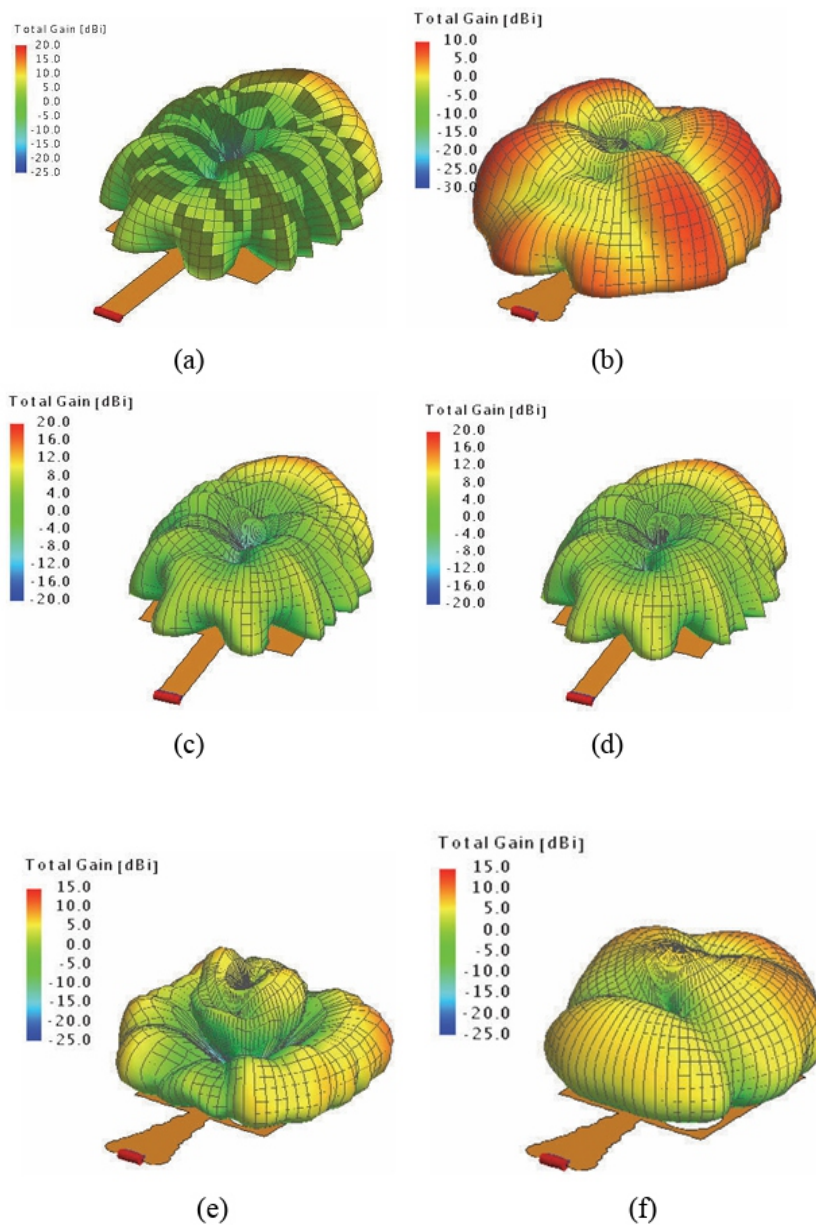


Fig. 3 – 3D total gain plots of microstrip antenna in x-y plane for (a) conventional antenna at resonant frequency (b) modified antenna at resonant frequency © conventional antenna at upper frequency (d) conventional antenna at lower frequency (e) modified antenna at upper frequency (f) modified antenna at lower frequency.

The current distribution result at the resonant frequencies for the conventional and modified antennas is presented (Fig. 5). For the conventional antenna, it observed that the current distribution has a high magnitude along the feed line (Fig. 5a). Applied the proposed modifications cause a change in patch geometry and influence the current distribution in a radiator patch (Fig. 5b).

Changing the current flow in the patch has been an influence on the value of the resonant frequency. On the other hand, Impedance matching plays an essential role in the antenna performance. The simulated results show that the impedance matching characteristics of the modified antenna (Fig. 6). It achieved good impedance performance close to 50Ω as comparing with the conventional antenna (Table 3).

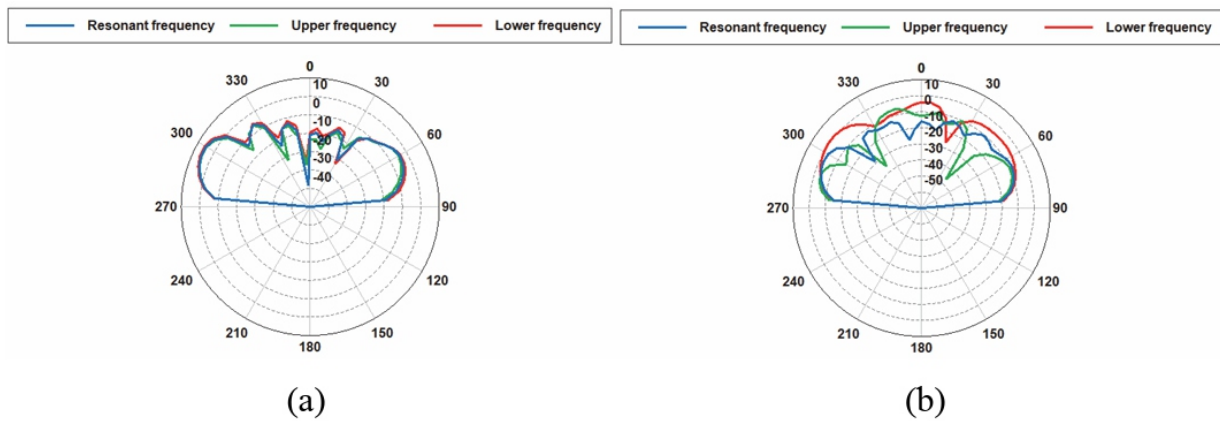


Fig. 4 – Polar gain results of microstrip planar antenna at: (a) conventional antenna; (b) modified antenna.

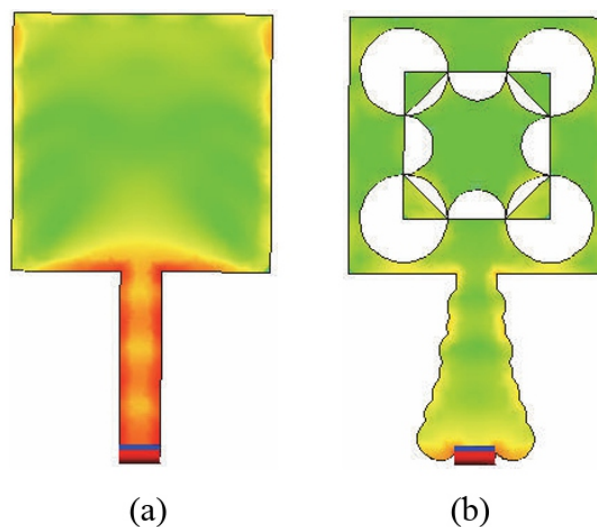


Fig. 5 – Current distribution results produced: (a) conventional antenna at 17.16 GHz; (b) modified antenna at 16.4 GHz.

Table 3 Impedance matching results.

Antenna	Resonant frequency (GHz)	Impedance matching (Ω)
Conventional	17.16	38.8
Modified	16.4	51.8

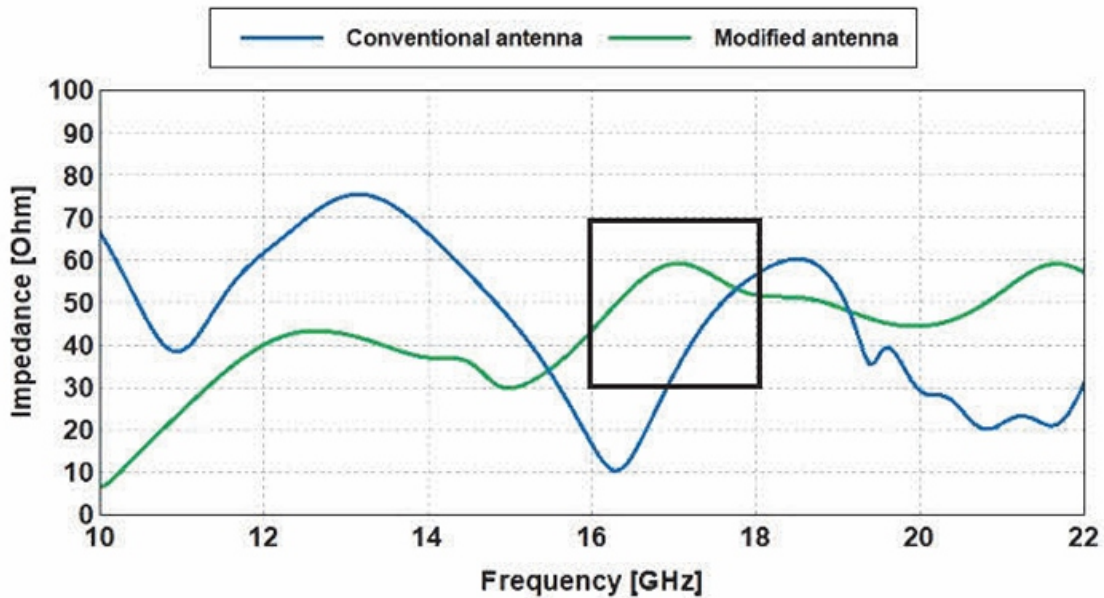
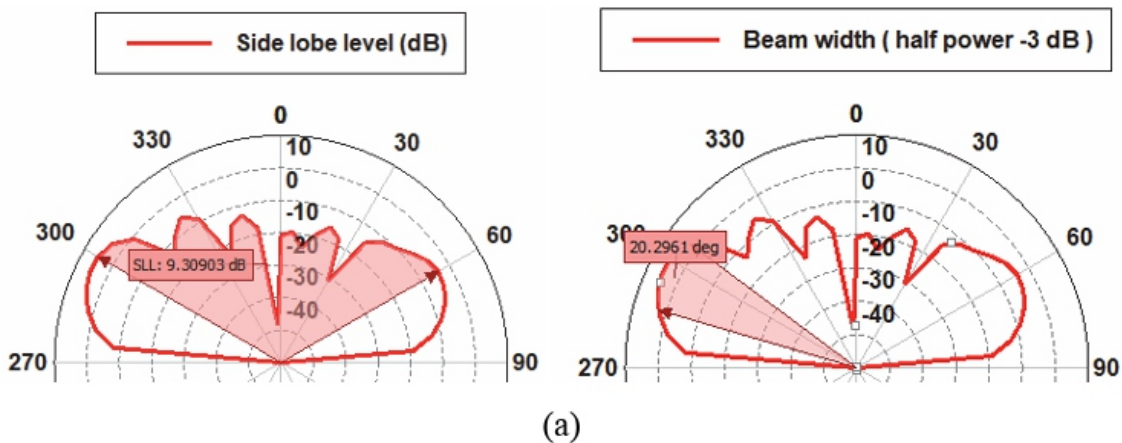


Fig. 6 – Impedance matching results for the conventional and modified antennas.

The sidelobe level is another parameter that is studied in this paper, which is usually represented as the unwanted radiation in undesired directions. It observed that SLL had been reduced to 5.72 dB at the resonant frequency of the modified antenna. Besides, the radiation patterns of the proposed antennas are also characterized by their beamwidths. Beamwidth is slightly decreased to 20.15 deg as compared with its result of the conventional antenna. Results of SLL and beamwidth for both antennas are presented in polar form (Fig. 7)



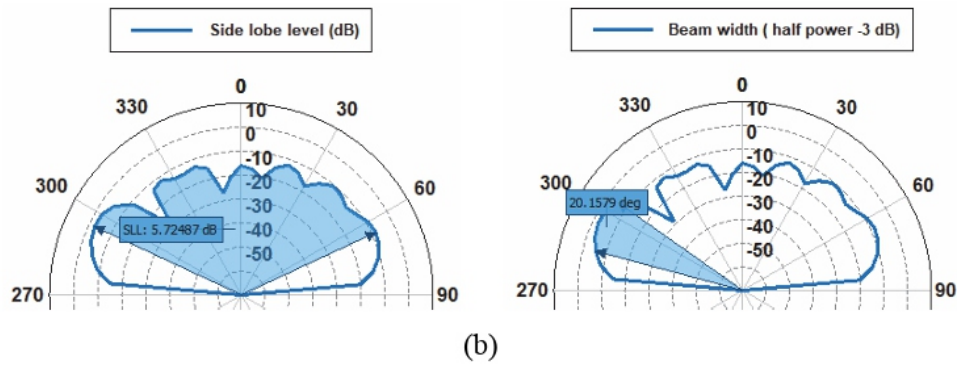


Fig. 7 – SLL and beamwidth at a resonant frequency of: (a) conventional antenna (b) modified antenna.

4 Experimental Results

The performance behaviour of the proposed antenna after modified has been verified through fabricated it and tested experimentally. The fabricated antenna has an impedance bandwidth of 10.02 GHz with an operating frequency range from 11.58 GHz to 21.6 GHz. The tested antenna is resonating at 16.56 GHz with a minimum reflection coefficient of -52.4 dB (Fig. 7). Results show that a satisfactory agreement with the simulation results.

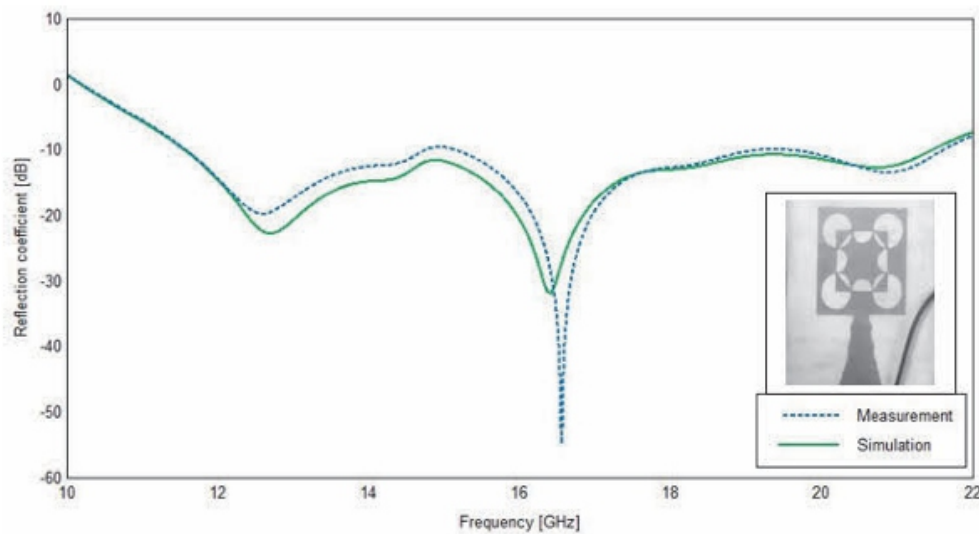


Fig. 7 – Top view of the fabricated antenna with a comparison of return losses between the measurement and simulation results.

6 Conclusion

A modified microstrip antenna for Ku/K band applications is presented and discussed theoretically and experimentally. Modifications have included the structure of the feed line and radiator patch. The bandwidth of the modified antenna has been improved to 9880 MHz, and the reflection coefficient has been minimized attained to -31.81 dB at the resonant frequency of a modified antenna. Other parameters have been studied, such as gain, impedance matching, sidelobe level, and beamwidth. The proposed antennas have been simulated and analyzed using commercial software (FEKO) based on the method of moment solver (MoM).

7 References

- [1] Y. Cui, Q. Zhou, X. Zhang, D. Shen, Y. Zhou: *A Novel Multiple-Stub Ultra-Wideband Antenna*, *Proceedings of the International Workshop on Antenna Technology: Small Antennas, Innovative Structures, and Applications (iWAT)*, Athens, Greece, March 2017, pp. 229 – 232.
- [2] R. Yadav: *Antenna and Wave Propagation*, 1st edition, Phi Learning Pvt. Ltd, New Delhi, India, 2011.
- [3] C. Balanis: *Antenna Theory – Analysis and Design*, 2nd edition, Wiley, New York, USA, 1997.
- [4] P.C. Aparna: *Wide Band U Shaped Patch Antenna for Wireless Applications*, *Proceedings of the International Conference on Wireless Communications, Signal Processing and Networking (WiSPNET)*, Chennai, India, March 2016, pp. 232 – 235.
- [5] A.S.W. Ghattas, E.E.M. Khaled: *A Compact Ultra-Wideband Microstrip Patch Antenna Designed for Ku/K Bands Applications*, *Proceedings of the Japan-Africa Conference on Electronics, Communications and Computers (JAC-ECC)*, Alexandria, Egypt, December 2017, pp. 61 – 64.
- [6] R. Mishra, J. Jayasinghe, R. Gaurav Mishra, P. Kuchhal: *Design and Performance Analysis of a Rectangular Microstrip Line Feed Ultra-Wide Band Antenna*, *International Journal of Signal Processing, Image Processing and Pattern Recognition*, Vol. 9, No. 6, July 2016, pp. 419 – 426.
- [7] R. Gaurav Mishra, R. Mishra, P. Kuchhal: *Design of Broadband Monopole Microstrip Antenna Using Rectangular Slot*, *Proceedings of the International Conference on Intelligent Communication, Control and Devices*, Dehradun, India, April 2016, pp. 683 – 688.
- [8] R. Mishra, R. Gaurav Mishra, P. Kuchhal: *Analytical Study on the Effect of Dimension and Position of Slot for the Designing of Ultra-Wide Band (UWB) Microstrip Antenna*, *Proceedings of the International Conference on Advances in Computing, Communications and Informatics (ICACCI)*, Jaipur, India, September 2016, pp. 488 – 493.
- [9] R. Mishra, P. Kuchhal, A. Kumar: *Effect of Height of the Substrate and Width of the Patch on the Performance Characteristics of Microstrip Antenna*, *International Journal of Electrical and Computer Engineering*, Vol. 5, No. 6, December 2015, pp. 1441 – 1445.
- [10] R. Gaurav Mishra, R. Mishra, P. Kuchhal, N. Prasanthi Kumari: *Design and Analysis of CPW-Fed Microstrip Patch Antennas for Wideband Applications*, *Proceedings of the International Conference on Inventive Computing and Informatics (ICICI)*, Coimbatore, India, November 2017, pp. 651 – 654.
- [11] N. Ripin, S.N.C. Yusoff, A.A. Sulaiman, N.E.A. Rashid, M.F. Hussin: *Enhancement of Bandwidth through I - Shaped Defected Ground Structure*, *Proceedings of the IEEE International RF and Microwave Conference (RFM)*, Penang, Malaysia, December 2013, pp. 477 – 481.
- [12] C.- M. Luo, J.- S. Hong, L.- L. Zhong: *Isolation Enhancement of a Very Compact UWBMIMO Slot Antenna with Two Defected Ground Structures*, *IEEE Antennas and Wireless Propagation Letters*, Vol. 14, April 2015, pp. 1766 – 1769.
- [13] K.H. Chiang, K.W. Tam: *Microstrip Monopole Antenna with Enhanced Bandwidth Using Defected Ground Structure*, *IEEE Antennas and Wireless Propagation Letters*, Vol. 7, September 2008, pp. 532 – 535.
- [14] E. Sarva Rameswarudu, P.V. Sridevi: *Bandwidth Enhancement Defected Ground Structure Microstrip Patch Antenna for K and Ka Band Applications*, *Proceedings of the 2nd International Conference on Advances in Electrical, Electronics, Information, Communication and Bio-Informatics (AEEICB)*, Chennai, India, February 2016, pp. 407 – 410.
- [15] S. Arif Ali, D. Jhanwar, D. Mathur: *Design of a Compact Triple Band-Notch Flower-Shaped Hexagonal Microstrip Patch Antenna*, *Proceedings of the International Conference on Information Technology (InCITe) - The Next Generation IT Summit on the Theme – Internet of Things: Connect your Worlds*, Noida, India, October 2016, pp. 293 – 298.

-
-
- [16] K. Anusudha, M. Karmugil: *Design of Circular Microstrip Patch Antenna for Ultra Wideband Applications*, *Proceedings of the International Conference on Control, Instrumentation, Communication and Computational Technologies (ICCICCT)*, Kumaracoil, India, December 2016, pp. 304 – 308.
- [17] H.S. Mewara, R. Kumawat, M.M. Sharma: *Design and Analysis of an Ultra-Wide Band Antenna Consisting of Extra Radiating Patch with Bandwidth Enhancement and Band Notch Characteristics*, *Proceedings of the International Conference on Recent Advances and Innovations in Engineering (ICRAIE)*, Jaipur, India, December 2016, pp. 1 – 5.
- [18] G. Aishvarya Devi, J. Aarthi, P. Bhargav, R. Pandeewari, M. Ananda Reddy, R. Samson Daniel: *UWB Frequency Reconfigurable Patch Antenna for Cognitive Radio Applications*, *Proceedings of the IEEE International Conference on Antenna Innovations & Modern Technologies for Ground, Aircraft and Satellite Applications (iAIM)*, Bangalore, India, November 2017, pp. 1 – 4.
- [19] A. Sarma, K. Sarmah, S. Goswami, K. Kumar Sarma, S. Baruah: *DGS Based Planer UWB Antenna with Band Rejection Features*, *Proceedings of the International Conference on Wireless Communications, Signal Processing and Networking (WiSPNET)*, Chennai, India, March 2017, pp. 2640 – 2644.
- [20] S. Feng, M.P. Jin: *Broad-Band Cavity-Backed and Probe-Fed Microstrip Phased Array Antenna in X-Band*, *Proceedings of the IEEE International Symposium on Antennas and Propagation & USNC/URSI National Radio Science Meeting*, San Diego, USA, July 2017, pp. 511 – 512.

Instructions for Authors

Essentials for Publishing in this Journal

- 1 Submitted articles should not have been previously published or be currently under consideration for publication elsewhere.
- 2 Conference papers may only be submitted if the paper has been completely re-written (taken to mean more than 50%) and the author has cleared any necessary permission with the copyright owner if it has been previously copyrighted.
- 3 All our articles are refereed through a double-blind process.
- 4 All authors must declare they have read and agreed to the content of the submitted article and must sign a declaration correspond to the originality of the article.

Submission Process

All articles for this journal must be submitted using our online submissions system. <http://enrichedpub.com/> . Please use the Submit Your Article link in the Author Service area.

Manuscript Guidelines

The instructions to authors about the article preparation for publication in the Manuscripts are submitted online, through the e-Ur (Electronic editing) system, developed by **Enriched Publications Pvt. Ltd.** The article should contain the abstract with keywords, introduction, body, conclusion, references and the summary in English language (without heading and subheading enumeration). The article length should not exceed 16 pages of A4 paper format.

Title

The title should be informative. It is in both Journal's and author's best interest to use terms suitable. For indexing and word search. If there are no such terms in the title, the author is strongly advised to add a subtitle. The title should be given in English as well. The titles precede the abstract and the summary in an appropriate language.

Letterhead Title

The letterhead title is given at a top of each page for easier identification of article copies in an Electronic form in particular. It contains the author's surname and first name initial .article title, journal title and collation (year, volume, and issue, first and last page). The journal and article titles can be given in a shortened form.

Author's Name

Full name(s) of author(s) should be used. It is advisable to give the middle initial. Names are given in their original form.

Contact Details

The postal address or the e-mail address of the author (usually of the first one if there are more Authors) is given in the footnote at the bottom of the first page.

Type of Articles

Classification of articles is a duty of the editorial staff and is of special importance. Referees and the members of the editorial staff, or section editors, can propose a category, but the editor-in-chief has the sole responsibility for their classification. Journal articles are classified as follows:

Scientific articles:

1. Original scientific paper (giving the previously unpublished results of the author's own research based on management methods).
2. Survey paper (giving an original, detailed and critical view of a research problem or an area to which the author has made a contribution visible through his self-citation);
3. Short or preliminary communication (original management paper of full format but of a smaller extent or of a preliminary character);
4. Scientific critique or forum (discussion on a particular scientific topic, based exclusively on management argumentation) and commentaries. Exceptionally, in particular areas, a scientific paper in the Journal can be in a form of a monograph or a critical edition of scientific data (historical, archival, lexicographic, bibliographic, data survey, etc.) which were unknown or hardly accessible for scientific research.

Professional articles:

1. Professional paper (contribution offering experience useful for improvement of professional practice but not necessarily based on scientific methods);
2. Informative contribution (editorial, commentary, etc.);
3. Review (of a book, software, case study, scientific event, etc.)

Language

The article should be in English. The grammar and style of the article should be of good quality. The systematized text should be without abbreviations (except standard ones). All measurements must be in SI units. The sequence of formulae is denoted in Arabic numerals in parentheses on the right-hand side.

Abstract and Summary

An abstract is a concise informative presentation of the article content for fast and accurate Evaluation of its relevance. It is both in the Editorial Office's and the author's best interest for an abstract to contain terms often used for indexing and article search. The abstract describes the purpose of the study and the methods, outlines the findings and state the conclusions. A 100- to 250-Word abstract should be placed between the title and the keywords with the body text to follow. Besides an abstract are advised to have a summary in English, at the end of the article, after the Reference list. The summary should be structured and long up to 1/10 of the article length (it is more extensive than the abstract).

Keywords

Keywords are terms or phrases showing adequately the article content for indexing and search purposes. They should be allocated heaving in mind widely accepted international sources (index, dictionary or thesaurus), such as the Web of Science keyword list for science in general. The higher their usage frequency is the better. Up to 10 keywords immediately follow the abstract and the summary, in respective languages.

Acknowledgements

The name and the number of the project or programmed within which the article was realized is given in a separate note at the bottom of the first page together with the name of the institution which financially supported the project or programmed.

Tables and Illustrations

All the captions should be in the original language as well as in English, together with the texts in illustrations if possible. Tables are typed in the same style as the text and are denoted by numerals at the top. Photographs and drawings, placed appropriately in the text, should be clear, precise and suitable for reproduction. Drawings should be created in Word or Corel.

Citation in the Text

Citation in the text must be uniform. When citing references in the text, use the reference number set in square brackets from the Reference list at the end of the article.

Footnotes

Footnotes are given at the bottom of the page with the text they refer to. They can contain less relevant details, additional explanations or used sources (e.g. scientific material, manuals). They cannot replace the cited literature.

The article should be accompanied with a cover letter with the information about the author(s): surname, middle initial, first name, and citizen personal number, rank, title, e-mail address, and affiliation address, home address including municipality, phone number in the office and at home (or a mobile phone number). The cover letter should state the type of the article and tell which illustrations are original and which are not.